
Since January 2020 Elsevier has created a COVID-19 resource centre with free information in English and Mandarin on the novel coronavirus COVID-19. The COVID-19 resource centre is hosted on Elsevier Connect, the company's public news and information website.

Healthcare Analytics 3 (2023) 100157

Contents lists available at ScienceDirect

Healthcare Analytics

journal homepage: www.elsevier.com/locate/health

# A bifurcation analysis and model of Covid-19 transmission dynamics with post-vaccination infection impact

Oke I. Idisi [a,*], Tunde T. Yusuf [a], Kolade M. Owolabi [a], Bolanle A. Ojokoh [b]

[a] Department of Mathematical Sciences, Federal University of Technology, Akure, P.M.B. 704, Ondo State, Nigeria
[b] Department of Information Systems, Federal University of Technology, Akure, P.M.B. 704, Ondo State, Nigeria

ARTICLE INFO

Dataset link: https://ourworldindata.org/coronavirus/country/Nigeria

*Keywords:*
Stability analysis
Backward bifurcation
Sensitivity analysis
Coronavirus
Control reproduction number
Metzler matrix

ABSTRACT

SARS COV-2 (Covid-19) has imposed a monumental socio-economic burden worldwide, and its impact still lingers. We propose a deterministic model to describe the transmission dynamics of Covid-19, emphasizing the effects of vaccination on the prevailing epidemic. The proposed model incorporates current information on Covid-19, such as reinfection, waning of immunity derived from the vaccine, and infectiousness of the pre-symptomatic individuals into the disease dynamics. Moreover, the model analysis reveals that it exhibits the phenomenon of backward bifurcation, thus suggesting that driving the model reproduction number below unity may not suffice to drive the epidemic toward extinction. The model is fitted to real-life data to estimate values for some of the unknown parameters. In addition, the model epidemic threshold and equilibria are determined while the criteria for the stability of each equilibrium solution are established using the Metzler approach. A sensitivity analysis of the model is performed based on the Latin Hypercube Sampling (LHS) and Partial Rank Correlation Coefficients (PRCCs) approaches to illustrate the impact of the various model parameters and explore the dependency of control reproduction number on its constituents parameters, which invariably gives insight on what needs to be done to contain the pandemic effectively. The foregoing notwithstanding, the contour plots of the control reproduction number concerning some of the salient parameters indicate that increasing vaccination coverage and decreasing vaccine waning rate would remarkably reduce the value of the reproduction number below unity, thus facilitating the possible elimination of the disease from the population. Finally, the model is solved numerically and simulated for different scenarios of disease outbreaks with the findings discussed.

## 1. Introduction

Infectious diseases modeling is a common tool used in studying the spread of communicable diseases, forecasting the future course of a disease outbreak, and evaluating strategies for controlling an epidemic [1]. Over the years, infectious disease agents like viruses, bacteria, fungi, protozoa, and helminthes have caused several diseases which have invaded the world resulting into a number of disease outbreaks [2]. Some of the recent ones are Ebola, Swine flu, Zika virus, Dengue fever, Yellow fever, MERS CoV, Monkey Pox, and more recently, Coronavirus (COVID-19) which wreaked havoc on the entire world.

Towards the end of year 2019, the emergence of Coronavirus sprung a sudden and disastrous outbreak across countries of the world causing several deaths and economy lock-down in many countries across the globe. The outbreak of Coronavirus was first recorded in China, precisely in Wuhan, Hubei province, on December 31 2019 [3,4]. Few days after, on 30th January, 2020 about 307,736 persons were confirmed infected with the virus and 12,167 suspected cases were reported in China while 82 persons were confirmed in 18 other countries. In the same day, World Health Organization declared the SARS-CoV-2 (COVID-19) outbreak as a Public Health Emergency of International Concern (PHEIC) [5–8]. As at 10th of November 2022, the pandemic has resulted into 639,023,177 confirmed cases and 6,610,754 deaths globally [9,10], while in Nigeria a total of 266,138 confirmed cases with 3155 deaths has been reported [11]. Due to the outbreak of Coronavirus, several policies and Non-Pharmaceutical Intervention (NPI) measures have been proposed and implemented globally ranging from contact tracing, washing of hands, social distancing, lock down, isolation, wearing of face mask, and recently, administration of vaccines to curtail the disease incidence and its spread [8,12]. Coronavirus is an enveloped and positive-sense single-stranded RNA (+ssRNA) virus which can be transmitted to an individual via direct contact with contaminated surface or droplets produced from the respiratory system of infected persons [8]. The transmission of the disease occur often during coughing or sneezing, and through inhalation of respiratory droplets

* Corresponding author.
*E-mail address:* idisioke@gmail.com (O.I. Idisi).

https://doi.org/10.1016/j.health.2023.100157
Received 20 December 2022; Received in revised form 1 March 2023; Accepted 4 March 2023

from asymptomatic and symptomatic infected humans. The incubation period of Coronavirus is estimated to range between 0 and 14 days, which is regarded as the minimum period for an exposed individuals to be quarantined [13,14]. Moreover, most of the infected individuals exhibit no clinical symptoms or show mild symptoms like dry cough, high fever, body ache, and breathing difficulties. In more severe cases, infection can cause pneumonia, kidney failure, and complication in the respiratory system [6,7,15,16].

Currently, there are no certified anti-retrovirus drugs for the treatment of the disease. However, infected individuals are medically treated in the hospitals based on the symptoms they exhibit and they eventually recover from the disease. Moreover, a number of effective vaccines have been developed to protect people from been infected. Some of the effective popular Covid-19 vaccine are Oxford Astra-Zeneca, Moderna, and Pfizer- BioNTech. As at 17th November 2021, about 7.45 billion COVID-19 vaccine doses had been administered worldwide, with 51.5% of the global population having received at least one dose of COVID-19 vaccine While 28.85 million vaccines were then being administered daily, though only 4.5% of people in low-income countries had received at least a first dose of the COVID-19 vaccine [17,18].

Prior to the development of COVID-19 vaccines, several mathematical models were developed and used to study the transmission dynamics of COVID-19 while equally assessing the impact of the different proposed control strategies on the spread of the disease [4,6,7,14,19–33]. For instance, some authors examined the impact of using the NPI measures on containing the disease. The findings from these works show that these NPI measures will only be effective if the compliance, particularly in public's spaces, is significantly high [25,34]. Based on slightly different perspectives, Tang et al. Giordano et al. and Ngonghala et al. demonstrate from their studies that timely detection of the infected individuals cum immediate hospitalization/quarantining coupled with intensive medical treatment for the identified infected patients would remarkably help in reducing the spread of the disease [7,14,21]. Nevertheless, findings from the works of Ivora et al. [30] and Idisi et al. [35] reveals that the undetected cases of Covid-19 individuals are the possible super-spreaders of the disease. The foregoing suggests that measures which will help timely detect infected Covid-19 individuals would be very useful in fight against the epidemic. On the otherhand, with the advent of Covid-19 vaccine, majority of the studies on Covid-19 dynamics which incorporate impact of the vaccine opined that the availability of vaccine against Covid-19 infection is a laudable one but the desired result will only be accomplished if the vaccine efficacy is remarkably high and the coverage for the administration of the vaccine is well above average (See [16,36,37]).

In recent times, several researchers have developed and suggested efficient techniques to figure out real and approximate solutions of the differential equation involving fractional operators and some of the commonly used operators are Riemann–Liouville, Caputo, Caputo–Fabrizio, Katugampola, Atangana–Baleanu to gain insight into the dynamic of corona virus disease [38–40,40–50]. For instant Alam Khan et al. [40]. develop a fractional order epidemic model for COVID-19 in the sense of Caputo operator, focusing on the effective contacts among the population and environmental impact to analyze the disease dynamics. To achieve it, they initially consider the classical integer model studied and thereafter generalize by introducing the Caputo fractional derivative. In same approach Sadia et al. [44] model the impact of the vaccine on the COVID-19 epidemic transmission via fractional derivative and adopt Adams–Bashforth–Moulton method, to obtain the approximate solution of the fractional-order COVID-19 model. The model numerical simulation was conducted with real data from Tunisia and they concluded from the study that, advancing the campaign of vaccination would be very beneficial in controlling the spread of the disease. Okundalaye et al. [46] proposed a time-fractional model for the SEIR COVID-19 mathematical model to predict the trend of COVID-19 epidemic in China. They adopt Multistage Optimal Homotopy Asymptotic Method (MOHAM) to solve their model for a closed-form series solution and compared with other analytical approximation method (OHAM, LHAM and HAM). From their findings, they concluded that (MOHAM) procedure is effective and has a distinct advantage over (OHAM, LHAM and HAM) approximation methods. Weiyuan et al. [43] proposed a two-side fractional generalized SEIR model to investigate spread and dynamics of COVID-19 in US. numerical tests reveal that when compared with integer-order and left-hand side fractional models, the model with both left-hand side fractional derivative and right-hand side fractional integral terms has a better forecast ability for the epidemic trend of COVID-19.

With reference to current information on COVID-19 [9,51], there has been a gap in understanding of the spread and dynamics of Coronavirus disease due to its novelty. Contrary to the initial public opinions, it has been reported that individuals who recovered from Coronavirus diseases can be reinfected unless they take adequate precautionary measures; individuals who have tested positive to the disease but are yet to display any of its symptoms (Pre-symptomatic) can infect others while individuals vaccinated against COVID-19 but discontinue adherence to Covid-19 preventive protocols or their vaccine-conferred immunity wanes can be infected with the disease. However, these gaps are not completely captured in majority of the earlier studies on Covid-19 [16,36,37]. Nevertheless, it is our aim in this paper to fill these research gaps as much as possible by developing a deterministic model which incorporates susceptibility of recovered and vaccinated individuals to reinfection as well as infectiousness of individuals in the pre-symptomatic phase in the spread of the disease. In order to show the reliability of our model, we fit the epidemic curve using Nigeria COVID-19 cases report, [11], estimate some model parameters for COVID-19 epidemic in Nigeria, and simulate the model to capture the Nigeria Covid-19 scenario. This paper is organized as follows: The epidemic deterministic model is developed and analyzed in Sections 2 and 3, respectively. In Section 5, parameter estimation cum model fitting are conducted and the analysis is presented. The model simulation and detailed discussion of our findings is presented in Section 6 while the concluding remarks is given in last section.

## 2. Methodology

### 2.1. Model formulation

The proposed model is based on the transmission dynamics of COVID-19 disease with emphasis on the dominant alpha strain of the disease. The total population at time t is denoted by $N(t)$; which is subdivided into Susceptible S(t), Vaccinated $V(t)$, Exposed $E(t)$, Asymptomatic $I_a(t)$, Symptomatic $I_s(t)$, Hospitalized $H(t)$, and Recovered $R(t)$ compartments. Thus,

$$N(t) = S(t) + V(t) + E(t) + I_a(t) + I_s(t) + H(t) + R(t).$$

Here, we considered COVID-19 transmission dynamics model described in [10,11] which is based on the facts that infection occurs only when individuals violate COVID-19 preventive protocols (wearing of face mask or keeping distance of at-least 2 m) and keep close contact with infected individuals either in the asymptomatic, symptomatic or hospitalized individuals class. Also, it is assumed that vaccinated individuals who engage in unprotected contacts with infectious Covid-19 individuals can be infected with the disease. The foregoing notwithstanding, based on recent reality, the proposed model assumes that individuals in the susceptible compartment ($S$) are exposed to the Covid-19 infection at effective infection rate $\beta_1$ while parameters $\omega, s\,(0 < (\omega, s) < 1)$ confer some level of protection on individuals who adhere to wearing of face mask and maintaining social distance in the public, while $\eta, \varepsilon$ are the modification parameters $(0 < \eta, \varepsilon < 1)$ that account for a reduction in the infectiousness of individuals in the infectious classes. The vaccinated class ($V$) population is increased at the rate $\rho$ per unit time and these vaccinated individuals can be infected at an effective infection rate $\sigma$ by individuals in the infectious classes while the infected

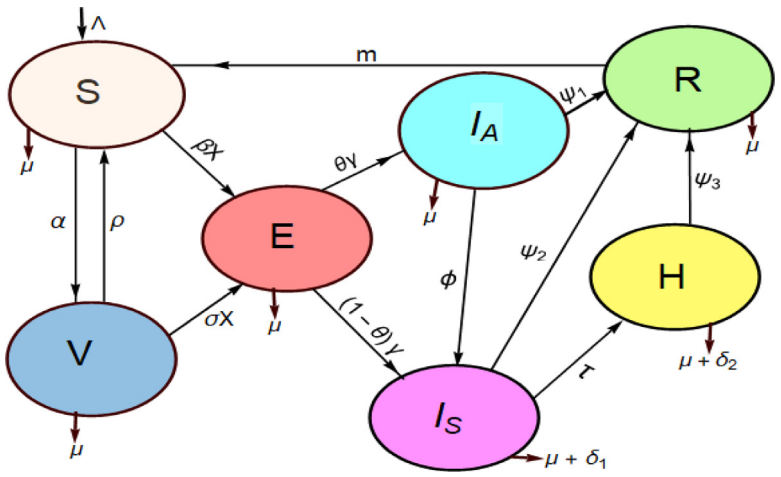


**Fig. 1.** Schematic Diagram for the proposed Model.

individuals with COVID-19 disease then proceed to the exposed class ($E$). From the exposed compartment, a proportion ($\theta\gamma$) of individuals in the class progress into the asymptomatic infectious compartment ($I_a$) while a proportion $(1-\theta)\gamma I_S$ enter into the symptomatic compartment ($I_s$). However, there is a further increase in this class population as a proportion ($\phi$) of individuals in the class later exhibit clinical symptoms after incubation period, thus progress to the symptomatically infected class ($I_s$). In addition, a proportion ($\tau$) of individuals in the class (who were identify via contact tracing, or voluntarily medical test) proceed to the Hospitalized/Self Isolation compartment ($H$). Individuals who recovered from COVID-19 disease at rate of $\psi_1, \psi_2, \psi_3$ respectively then became members of the recovered compartment ($R$). Furthermore, individuals who lost their temporary immunity equally returns to susceptible class at a rate $m$. Besides, disease-induced death rates for $I_s$ and $H$ classes are taken as $\delta_1, \delta_2$ respectively. Nevertheless, there is a further decrease in population across all the compartments due to natural death rate $\mu$. The proposed model dynamics is depicted by the flow diagram in Fig. 1 while the state variables and the model parameters are described in Table 1. The model equations is given by the following system of non-linear ordinary differential equations:

$$\begin{aligned}
\frac{dS}{dt} &= \Lambda + mR + \alpha V - \beta_1(1-w-s)\frac{(I_a+\eta I_s+\varepsilon H)S}{N} - (\mu+\rho)S,\\
\frac{dV}{dt} &= \rho S - \sigma(1-w-s)\frac{(I_a+\eta I_s+\varepsilon H)V}{N} - (\mu+\alpha)V,\\
\frac{dE}{dt} &= \beta_1(1-w-s)\frac{(I_a+\eta I_s+\varepsilon H)S}{N}\\
&\quad + \sigma(1-w-s)\frac{(I_a+\eta I_s+\varepsilon H)V}{N} - (\gamma+\mu)E,\\
\frac{dI_a}{dt} &= (1-\theta)\gamma E - (\psi_1+\phi+\mu)I_a,\\
\frac{dI_s}{dt} &= \theta\gamma E + \phi I_a - (\psi_2+\tau+\delta_1+\mu)I_s,\\
\frac{dH}{dt} &= \tau I_s - (\psi_3+\delta_2+\mu)H,\\
\frac{dR}{dt} &= \psi_1 I_a + \psi_2 I_s + \psi_3 I_H - (\mu+m)R.
\end{aligned} \tag{1}$$

It is pertinent to mention that the model (1) is written in compact form in order to facilitate the qualitative analysis of the model. Thus, the compact model equations on which the analysis will be premised is presented below:

$$\begin{aligned}
\frac{dS}{dt} &= \Lambda + mR + \alpha V - \beta XS - (\mu+\rho)S,\\
\frac{dV}{dt} &= \rho S - \sigma XV - (\mu+\alpha)V,\\
\frac{dE}{dt} &= \beta XS + \bar{\sigma}XV - k_1 E,\\
\frac{dI_a}{dt} &= (1-\theta)\gamma E - (k_2+\phi)I_a,\\
\frac{dI_s}{dt} &= \theta\gamma E + \phi I_a - k_3 I_s,\\
\frac{dH}{dt} &= \tau I_s - k_4 H,\\
\frac{dR}{dt} &= \psi_1 I_a + \psi_2 I_s + \psi_3 I_H - (\mu+m)R,
\end{aligned} \tag{2}$$

where $\beta = \beta_1(1-w-s)$, $\sigma = \sigma_1(1-w-s)$, $X = \frac{(I_a+\eta I_s+\varepsilon H)}{N}$, $k_1 = (\gamma+\mu)$, $k_2 = (\psi_1+\mu)$, $k_3 = (\psi_2+\delta_1+\tau+\mu)$, $k_4 = (\psi_3+\delta_2+\mu)$.

## 3. Model analysis

In this section, a detailed and rigorous analysis of the model is presented to gain insight into the dynamical features of the model.

### 3.1. Basic properties of the model

It is paramount to show that the proposed model has a solution and communicate practical sense. Thus, we show that the formulated model has well define solutions with unique solution confined within a positive invariant region, which makes the formulated model (2) to be well posed and epidemiological meaningful.

**Theorem 3.1.** *Let $\Gamma$ denote a rectangular region, model (2) with initial values $S(0) > 0, V(0) > 0, E(0) > 0, I_a(0) > 0, I_s(0) > 0, H(0) > 0, R(0) > 0$ exist,bounded, positively invariant and attracting for all $t > 0$*

### 3.2. Existence and uniqueness

**Proof.** We show that $\frac{\partial F_i}{\partial x_i}$, $i, j = 1 \ldots 6$ are continuous and bounded in $\mathcal{D}$.

Let $F_1 = \Lambda + mR + \alpha V - \bar{\beta}XS - (\mu+\rho)S$ from the first system of Eq. (1), differentiating with respect to the state variable, we have:

$$\begin{aligned}
\frac{\partial F_1}{\partial S} &= -\frac{\bar{\beta}X}{N} + \frac{\bar{\beta}XS}{N^2} - \mu - \rho, \quad \left|\frac{\partial F_1}{\partial S}\right| = \left|-\frac{\bar{\beta}X}{N}\right| + \left|\frac{\bar{\beta}XS}{N^2} - \mu - \rho\right| < \infty\\
\frac{\partial F_1}{\partial V} &= \alpha + \frac{\bar{\beta}XS}{N^2}, \quad \left|\frac{\partial F_1}{\partial V}\right| = \left|\alpha + \frac{\bar{\beta}XS}{N^2}\right| < \infty\\
\frac{\partial F_1}{\partial E} &= \frac{\bar{\beta}XS}{N^2}, \quad \left|\frac{\partial F_1}{\partial E}\right| = \left|\frac{\bar{\beta}XS}{N^2}\right| < \infty\\
\frac{\partial F_1}{\partial I_s} &= -\frac{\bar{\beta}\eta S}{N} + \frac{\bar{\beta}XS}{N^2}, \quad \left|\frac{\partial F_1}{\partial I_s}\right| = \left|-\frac{\bar{\beta}\eta S}{N}\right| + \left|\frac{\bar{\beta}XS}{N^2}\right| < \infty\\
\frac{\partial F_1}{\partial I_a} &= -\frac{\bar{\beta}S}{N} + \frac{\bar{\beta}XS}{N^2}, \quad \left|\frac{\partial F_1}{\partial I_a}\right| = \left|-\frac{\bar{\beta}S}{N}\right| + \left|\frac{\bar{\beta}XS}{N^2}\right| < \infty\\
\frac{\partial F_1}{\partial H} &= -\frac{\bar{\beta}\varepsilon S}{N} + \frac{\bar{\beta}XS}{N^2}, \quad \left|\frac{\partial F_1}{\partial H}\right| = \left|-\frac{\bar{\beta}\varepsilon S}{N}\right| + \left|\frac{\bar{\beta}XS}{N^2}\right| < \infty\\
\frac{\partial F_1}{\partial R} &= m + \frac{\bar{\beta}XS}{N^2}, \quad \left|\frac{\partial F_1}{\partial R}\right| = \left|m + \frac{\bar{\beta}XS}{N^2}\right| < \infty
\end{aligned} \tag{3}$$

its obvious that the partial derivatives of the whole system of equations exists, finite and bounded.

**Table 1**
Description of Variables and Parameters used in the Model (2).

| Variable | Interpretation |
|---|---|
| $S$ | Population of susceptible individuals |
| $V$ | Population of vaccinated individuals |
| $E$ | Population of Exposed individuals |
| $I_a$ | Population of asymptotically infectious individuals |
| $I_s$ | Population of symptomatically infectious individuals |
| $H$ | Population of hospitalized individuals |
| $R$ | Population of recovered individuals |
| **Parameter** | **Interpretation** |
| $\Lambda$ | Recruitment rates into the population |
| $m$, $\alpha$ | Immunity waning rate for individuals in $V(t)$ or $R(t)$ class respectively |
| $\gamma$ | Transmission rate of individuals from exposed compartment to symptomatic and asymptomatic compartment |
| $\rho$ | Vaccination rate of individuals |
| $\theta$ | Fraction of exposed that show clinical symptoms |
| $\delta_1, (\delta_2)$ | Disease mortality rate in symptomatic and Hospitalized population ($I_a$ & $H$) class |
| $\psi_1, (\psi_2, \psi_3)$ | Rate of recovery from ($I_a, I_s$ & $H$) class |
| $\phi$ | Population of pre-symptomatic infectious individuals (i.e., infected without symptoms but develop symptoms at the end of incubation period) |
| $\tau$ | Rate of transmission from $I_s$ to Hospitalized class |
| $\sigma$ | Effective infection rate for vaccinated individuals |
| $\beta_1$ | Effective infection rate for susceptible individuals |
| $w$ | Proportion of individual that uses face mask |
| $s$ | Proportion of individual that adhere to social distancing |
| $\eta, (\varepsilon)$ | Modification parameter for decrease on infectiousness in $I_s$,($H$) |
| $1/\mu$ | Human average life span |

### 3.3. Positivity and boundedness

For the model (2) to be epidemiologically meaningful, it is pertinent to show that all its state variables are non-negative for all time ($t$).

**Theorem 3.2.** *Given $S(0) \geq 0$, $V(0) \geq 0$, $E(0) \geq 0$, $I_a(0) \geq 0$, $I_s(0) \geq 0$, $H(0) \geq 0$, $R(0) \geq 0$. Then the solution $(S(t), V(t), E(t), I_a(t), I_s(t), H(t), R(t))$ of model (2) are positive at all $t > 0$.*

**Proof.** Let $t_1 = \sup(t > 0 | S > 0, V > 0, E > 0, I_a > 0, I_s > 0, H > 0, R > 0)$. From the first equation of (1) we have

$$\begin{aligned} \frac{dS}{dt} &= \Lambda + mR(t) + \alpha V(t) - \bar{\beta} X(t) S(t) - (\mu + \rho) S(t) \\ \frac{dS}{dt} &\geq \Lambda - (\bar{\beta} X(t) + \mu + \rho) S(t) \end{aligned} \tag{4}$$

The integrating factor is given as: $\exp\left(\int_0^t \bar{\beta} X(s) ds + (\mu + \rho) t\right)$

Multiplying the inequality (4) by the integrating factor, we obtain

$$\frac{d\left[S(t) \exp\left\{\int_0^t \bar{\beta} X(s) ds + (\mu + \rho) t\right\}\right]}{dt} \geq \Lambda \exp\left(\int_0^t (\bar{\beta} X(s) ds + \mu + \rho) t\right) \tag{5}$$

Solving inequality (5) we obtain

$$\begin{aligned} & S(t) \exp\left\{\int_0^t \bar{\beta} X(s) ds + (\mu + \rho) t\right\} - S(0) \\ & \geq \int_0^t \Lambda \exp\left\{\int_0^v (\bar{\beta} X(q) dq) + (\mu + \rho) v\right\} dv \end{aligned} \tag{6}$$

$$\begin{aligned} S(t) \geq S(0) & \exp\left\{-\int_0^t \bar{\beta} X(q) dq + (\mu + \rho) t\right\} \\ & + \exp\left\{-\int_0^t \bar{\beta} X(q) dq + (\mu + \rho) t\right\} \\ & \times \int_0^t \Lambda \exp\left\{\int_0^v (\bar{\beta}) X(q) dq + (\mu + \rho) v\right\} dv > 0 \end{aligned} \tag{7}$$

In a similarly pattern, it can be shown that:

$V > 0, E > 0, I_a > 0, I_s > 0, H > 0, R > 0$ in model (2); which implies that $S(t), V(t), E(t) I_s(t), I_a(t), H(t)$ and $R(t)$ are all non-negative for non-negative initial conditions.

### 3.4. Boundedness of the solution

**Theorem 3.3.** *All solutions $S(t), V(t), E(t) I_s(t), I_a(t), H(t)$ and $R(t)$ of model (2) are bounded.*

**Proof.** Adding all the equations of model system (2) gives:

$$\begin{aligned} \frac{dN}{dt} &= \Lambda - \mu N - \delta_1 I_s + \delta_2 H \\ \frac{dN}{dt} &\leq \Lambda - \mu N \end{aligned} \tag{8}$$

Solving Eq. (8) using standard comparison theorem; we illustrate the following steps:

$$\begin{aligned} \frac{dN(t)}{dt} &\leq \Lambda - \mu N \\ \frac{dN}{dt} + \mu N &\leq \Lambda \end{aligned} \tag{9}$$

The integrating factor is given as: $\exp^{\int \mu t}$; thus multiplying the inequality (9) by the integrating factor, we obtain

$$\begin{aligned} \int d\, e^{\mu t} N(t) &\leq \int \Lambda\, e^{\mu t}.dt \\ e^{\mu t} N(t) &\leq \frac{\Lambda}{\mu} e^{\mu t} + C \\ N(t) &\leq e^{-\mu t}\left(\frac{\Lambda}{\mu} e^{\mu t} + C\right) \end{aligned} \tag{10}$$

Using initial condition ($i.e.\ N(t) = N(0)$ *at* $t = 0$), it implies that

$$\begin{aligned} N(t) &\leq e^{-\mu t}\left[\frac{\Lambda}{\mu} e^{\mu t} + \left(N(0) - \frac{\Lambda}{\mu}\right)\right] \\ N(t) &\leq N(0) e^{-\mu t} + \frac{\Lambda}{\mu}\left(1 - e^{-\mu t}\right) \\ &\Rightarrow \lim_{t \to \infty} N(t) \leq \frac{\Lambda}{\mu} \end{aligned} \tag{11}$$

Hence, $\frac{\Lambda}{\mu}$ is the upper bound of $N(t)$, applying the comparison theorem as in [52], we have that $N(t) \leq \frac{\Lambda}{\mu}$, if $N(0) \leq \frac{\Lambda}{\mu}$. Thus, $\frac{\Lambda}{\mu}$ is the upper bound for the region $\Gamma$ and is positively invariant [53]. Further, if $N(t) > \frac{\Lambda}{\mu}$ then either the solution enters $\Gamma$ in finite time, or $N(t)$ approaches $\frac{\Lambda}{\mu}$ and the infected variables $E$, $I_a$, $I_s$, $H$, $R$ approach zero. Hence, it is sufficient to conclude that the set $\Gamma$ is positively invariant and all solutions of the model Eqs. (2) are non-negative and epidemiological well posed [54].

### 3.5. Disease free equilibrium (DFE)

At the equilibrium, we set LHS of the model equations to zeros and solve for the resulting system simultaneously to obtain the model Disease-free equilibrium (DFE) and the Endemic equilibrium. The model Disease-free equilibrium is given below:

$$\begin{aligned}\mathcal{E}_0 &= \{S^*, V^*, E^*, I_a^*, I_s^*, H^*, R^*\} \\ &= \left(\frac{(\mu+\alpha)\Lambda}{\mu(\rho+\alpha+\mu)}, \frac{\rho\Lambda}{\mu(\rho+\alpha+\mu)}, 0, 0, 0, 0, 0\right)\end{aligned} \tag{12}$$

### 3.6. Reproduction number

The control reproduction number ($R_{0V}$) of the model (2), measures the average number of new COVID-19 cases generated by a typical Covid-19 infectious individual introduced into a population where a certain fraction is protected (in presence of control measures i.e vaccination, and Non Pharmaceutical Interventions). However, the basic reproduction number $\mathcal{R}_0$ is derived by considering the worse case scenario where no preventive measures is implemented in the population and $\mathcal{R}_0$ is derived using the next generation matrix method as described in [55] based on model (2) evaluated at the model DFE given in Eq. (12). Consequently, the control reproduction number was computed with notation $F$ (for the new infection terms) and $V$ (for transfer terms) respectively given by

$$FV^{-1} = \begin{bmatrix} 0 & \frac{(\mu+\alpha)\beta+\rho\sigma}{\mu+\alpha+\rho} & \frac{[(\mu+\alpha)\beta+\rho\sigma]\eta}{\mu+\alpha+\rho} & \frac{[(\mu+\alpha)\beta+\rho\sigma]\epsilon}{\mu+\alpha+\rho} \\ 0 & 0 & 0 & 0 \\ 0 & 0 & 0 & 0 \\ 0 & 0 & 0 & 0 \end{bmatrix} \times \begin{bmatrix} \frac{1}{k_1} & 0 & 0 & 0 \\ \frac{(1-\theta)\gamma}{k_1(k_2)+\phi} & \frac{1}{k_2+\phi} & 0 & 0 \\ \frac{\gamma(k_2+\phi)}{k_1(k_2+\phi)k_3} & \frac{\phi}{(k_2+\phi)k_3} & \frac{1}{k_3} & 0 \\ \frac{\tau\gamma(k_2+\phi)}{k_1(k_2+\phi)k_3k_4} & \frac{\tau\phi}{(k_2+\phi)k_3k_4} & \frac{\tau}{k_3k_4} & \frac{1}{k_4} \end{bmatrix} \tag{13}$$

Now, we define the quantity $\mathcal{R}_{0V}$ as the spectral radius of the next generation matrix ($FV^{-1}$) which is obtained as stated below:

$$\mathcal{R}_{0V} = \rho(FV^{-1}) = \frac{\gamma\left[\beta(\mu+\alpha)+\rho\sigma\right]\left[k_3k_4(1-\theta)+k_4\eta(k_2\theta+\phi)+\tau\epsilon(k_2\theta+\phi)\right]}{k_1k_3k_4(\mu+\alpha+\rho)(k_2+\phi)} \tag{14}$$

where

$$\begin{aligned}\mathcal{R}_a &= \frac{\gamma(1-\theta)A_1}{(\mu+\alpha+\rho)k_1(k_2+\phi)}, \ \mathcal{R}_s = \frac{\gamma\eta(k_2\theta+\phi)A_1}{(\mu+\alpha+\rho)(k_2+\phi)k_1k_3}, \\ \mathcal{R}_h &= \frac{\epsilon\tau\gamma(k_2\theta+\phi)A_1}{(\mu+\alpha+\rho)k_1(k_2+\phi)k_3k_4}\end{aligned} \tag{15}$$

with $A_1 = (\mu+\alpha)\beta+\sigma\rho$

The quantity $\mathcal{R}_{0V}$ is the control reproduction number for model (2) which measures the average number of new COVID-19 cases generated by introducing a typical infectious individual into a susceptible population where a certain fraction of the populace adhere to NPI measures in public and/or are vaccinated against COVID-19. Moreover, $\mathcal{R}_{0V}$ is the sum of the constituent reproduction numbers associated with the number of new cases generated by asymptomatically-infectious individuals ($\mathcal{R}_a$), symptomatically infectious individuals ($\mathcal{R}_s$), and Hospitalized infectious individuals ($\mathcal{R}_h$).

### 3.7. Threshold analysis and vaccine impact

In this subsection, the potential impact of a single dose and a fractional dosing of the vaccine is analyzed. Based on the facts that it is often impracticable to vaccinate all susceptible individuals due to many reasons (e.g financial constraints, age of the recipient, belief, etc.).

It is therefore instructive to first of all assess the impact of vaccine on the spread of the disease. Let us recall that the control reproduction number in term of S and V is

$$\mathcal{R}_{0V} = \frac{(S^*\beta+V^*\sigma)\gamma\left[k_3k_4(1-\theta)+k_4\eta(k_2\theta+\phi)+\tau\epsilon(k_2\theta+\phi)\right]}{(S^*+V^*)(k_2+\phi)k_1k_3k_4}. \tag{16}$$

Considering the worse case scenario, where there is no public health control or mitigation measures implemented and the disease spreads in the population, then $V^* = 0$ and $S^* = N^*$. Therefore, the control reproduction number reduces to

$$\mathcal{R}_0 = \mathcal{R}_{0V}|_{V^*=0} = \frac{\gamma\beta\left[k_3k_4(1-\theta)+k_4\eta(k_2\theta+\phi)+\tau\epsilon(k_2\theta+\phi)\right]}{k_1(k_2+\phi)k_3k_4}. \tag{17}$$

So, $\mathcal{R}_{0V} \leq \mathcal{R}_0$, since $\frac{\beta(\alpha+\mu)+\rho\sigma}{\mu+\alpha+\rho} > 0$. Thus, vaccination of individuals will have positive impact in the community by reducing the value of the associated reproduction number $\mathcal{R}_0$. Furthermore, using a similar approach as employed in [56], the impact of vaccination can be analyzed qualitatively by differentiating $\mathcal{R}_{0V}$. with respect to the fraction of vaccinated individuals ($V$). It can be shown that

$$\frac{\partial\mathcal{R}_{0V}}{\partial V} = \frac{-S^*\gamma(\beta-\sigma)\left[k_3k_4(1-\theta)+k_4\eta(k_2\theta+\phi)+\tau\epsilon(k_2\theta+\phi)\right]}{(S^*+V^*)^2(k_2+\phi)k_1k_3k_4} < 0, \quad since \quad \beta > \sigma. \tag{18}$$

Therefore, $\mathcal{R}_{0V}$ is a decreasing function of $V$. The implication of the foregoing result is that vaccination will have a positive impact in COVID-19 disease control, since $\mathcal{R}_0$ is a measure of the marginal incidence of the disease which cumulatively constitutes the disease burden in the society.

## 4. Steady state analysis of ($\mathcal{E}_0$)

In order to eliminate COVID-19 disease independent of subpopulation of the model, it is necessary to show that the disease-free equilibrium (DFE) is locally and globally asymptotically stable. We adopt negativity of the real parts of the associated Jacobian Matrix approach to obtain the local stability and the Metzler approach described in [56], to establish the conditions for the globally asymptotically stability of DFE.

### 4.1. Local stability

**Theorem 4.1.** *The disease free equilibrium point is locally asymptomatically stable if the constituent* $\{R_a, R_s\} < 1$ *and unstable for* $\{R_a, R_s\} > 1$.

**Proof.** The Jacobian of the system (2) at the DFE point in (12) is given as (19) in Box I. Obviously it is clear, that the first two eigenvalues of Eq. (19) are negative ($-\kappa_4$ *and* $-(\mu+m)$) However we solve for the characteristic Polynomial as

$$P(\xi) = (\xi+\mu)(\xi+\mu+\alpha+\rho)\left[\xi^3 + a_x\xi^2 + a_y\xi + a_z\right],$$

where

$$\begin{aligned}a_x &= \kappa_1+\kappa_2+\kappa_3+\phi \\ a_y &= (\mu+\alpha+\rho)(1-R_a)+\kappa_3(\kappa_1+\kappa_2+\phi)-\gamma\eta\theta A \\ a_z &= (\kappa_2+\phi)(1-R_s)+\kappa_3(\kappa_2+\phi)(1-R_a)\end{aligned} \tag{20}$$

The third-order polynomial $P(\xi) = \xi^3+a_x\xi^2+a_y\xi+a_z$ has all roots in the open left half-plane if and only if $a_x$, $a_y$, *and* $a_z$ are positive. Moreover, in order to ensure that the quantity $a_xa_y - a_z$ is positive; it suffices that $\{R_a, R_s\} < 1$, which fulfills the condition of Routh–Hurwitz criteria. Thus, the Disease-free equilibrium is locally asymptotically stable (LAS).

$$J(E_0) = \begin{bmatrix} -(\mu+\rho) & \alpha & 0 & -\frac{\beta(\mu+\alpha)}{\mu+\alpha+\rho} & -\frac{\eta\beta(\mu+\alpha)}{\mu+\alpha+\rho} & -\frac{\epsilon\beta(\mu+\alpha)}{\mu+\alpha+\rho} & m \\ \rho & -(\alpha+\mu) & 0 & -\frac{\sigma\rho}{\mu+\alpha+\rho} & \frac{-\eta\sigma\rho}{\mu+\alpha+\rho} & -\frac{\epsilon\sigma\rho}{\mu+\alpha+\rho} & 0 \\ 0 & 0 & \kappa_1 & \frac{\beta(\mu+\alpha)+\sigma_1\rho}{\mu+\alpha+\rho} & \frac{\eta\left[\beta(\mu+\alpha)+\sigma_1\rho\right]}{\mu+\alpha+\rho} & \frac{\epsilon\left[\beta(\mu+\alpha)+\sigma_1\rho\right]}{\mu+\alpha+\rho} & 0 \\ 0 & 0 & (1-\theta)\gamma & -\kappa_2 & 0 & 0 & 0 \\ 0 & 0 & \theta\gamma & \phi & -\kappa_3 & 0 & 0 \\ 0 & 0 & 0 & 0 & \tau & -\kappa_4 & 0 \\ 0 & 0 & 0 & \psi_1 & \psi_2 & \psi_3 & -(\mu+m) \end{bmatrix} \tag{19}$$

**Box I.**

### 4.2. Global stability

To show the global asymptotical stability, of the disease free equilibria of the system represent by (2) we adopt the Metzler technique. The subsequent theorem yield to the desired result.

**Theorem 4.2.** *Considering the model system (2), let $\Gamma \subset \mathbb{R}_+^{n_1+n_2}$ be a positively invariant set. If*

1. *The system (2) is defined on the positively invariant set $\Gamma \subset \mathbb{R}_+^{n_1+n_2}$;*
2. *The sub-system $\dot{x_1} = A_1(x_1, 0).(x_1 - x_1^*)$ is globally asymptotically stable at the equilibrium $x^*$;*
3. *For any $x \in \Gamma$, the matrix $A_{22}(x)$ is Metzler irreducible;*
4. *There exist an upper bound matrix $\bar{A}_{22}$ for the set $\mathcal{M} = \{A_{22}(x)|x \in \Gamma\}$ with the property that either $A_{22}(x) \notin \mathcal{M}$ or if $A_{22}(x) \in \mathcal{M}$(i.e., $\bar{A}_{22} = \max_\Gamma \mathcal{M}$), then for $x^* \in \Gamma$ such that, $\bar{A}_{22} = A_{22}(x^*)$, then $x^* \in \mathcal{M}^7 \times \{0\}$(the DFE sub-manifold contains the points where the maximum is attained);*
5. *The stability modulus of $\bar{A}_{22}$ satisfies $\alpha(\bar{A}_{22}) \leq 0$;*

*Then, the associated disease free equilibrium is globally asymptotically stable in $\Gamma$.*

**Proof.** Given model (2) rewritten in pseudo-triangular form with the use of property of DFE, we have

$$\begin{cases} \dot{x_1} &= A_{11}(x).(x_1 - x_1^*) + A_{12}(x)x_2 \\ \dot{x_2} &= A_{22}(x)x_2 \end{cases} \tag{21}$$

where $x_1 = (S, V, R)^T$ represents the non transmitting compartment of model (2), $x_2 = (E, I_a, I_s, H)^T$ represents the infectious compartment of the model, $x_1^* = (S^*, V^*, R^*)^T$ is the DFE while

$$\begin{aligned} A_{11}(x) &= \begin{pmatrix} -(\mu+\rho) & \alpha & m \\ \rho & -(\mu+\alpha) & 0 \\ 0 & 0 & -(\mu+m), \end{pmatrix} \\ A_{12}(x) &= \begin{pmatrix} -\frac{\beta_1 S}{S+V} & -\frac{\beta_1\eta S}{S+V} & -\frac{\beta_1\epsilon S}{S+V} \\ -\frac{\sigma_1 V}{S+V} & -\frac{\sigma_1\eta V}{S+V} & -\frac{\sigma_1\epsilon V}{S+V}, \\ \psi_1 & \psi_2 & \psi_3, \end{pmatrix} \\ A_{22}(x) &= \begin{pmatrix} -\kappa_1 & \frac{\beta_1 S+\sigma_1 V}{S+V} & \frac{\eta\left[(S\beta_1)+\sigma_1 V\right]}{S+V} & \frac{\epsilon\left[S\beta_1+\sigma_1 V\right]}{S+V} \\ (1-\theta)\gamma & -(\kappa_2+\phi) & 0 & 0 \\ \theta\gamma & \phi & -\kappa_3 & 0 \\ 0 & 0 & \tau & -\kappa_4. \end{pmatrix} \end{aligned} \tag{22}$$

Recall that the model (2) is defined on a positive invariant domain given by $\Gamma$. Also, by direct computation, the eigenvalues of $A_{11}(x)$ are $\{-(\mu+\rho), -(\mu+\alpha), -(\mu+m)\}$ which are real and negative. Therefore, conditions 1 and 2 of 4.2 are satisfied. For condition 3 of 4.2, we show that a square matrix $A_{22}(x_2)$ is irreducible if and only if its diagraph is strongly connected. Fig. 2 is obtained by substituting the parameter

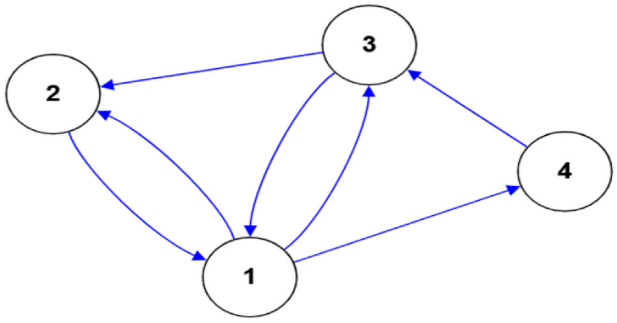


**Fig. 2.** Connected di-graph associated with the matrix $A_{22}(x)$.

baseline values as presented in Table 2 into Eq. (22) to obtain its adjacency matrix and using online platform https://graphonline.ru/en/create_graph_by_matrix to plot the associated digraph of the matrix $A_{22}(x)$ which is further verified at https://www.geeksforgeeks.org/check-if-a-directed-graph-is-connected-or-not/ using online version of C++ programme whose output indicate that the digraph is strongly connected. Thus condition (3) is satisfied.

Furthermore, since $S = \frac{\Lambda(\mu+\alpha)}{\mu(\mu+\alpha+\rho)}$ and $V = \frac{\Lambda\rho}{\mu(\mu+\alpha+\rho)}$, then the matrix

$$\bar{A}_{22}(x) = \begin{pmatrix} -\kappa_1 & \frac{\beta_1(\mu+\alpha)+\sigma_1\rho}{\mu+\alpha+\rho} & \frac{\eta\left[\beta_1(\mu+\alpha)+\sigma_1\rho\right]}{\mu+\alpha+\rho} & \frac{\epsilon\left[\beta_1(\mu+\alpha)+\sigma_1\rho\right]}{\mu+\alpha+\rho} \\ (1-\theta)\gamma & -\kappa_2 & 0 & 0 \\ \theta\gamma & \phi & -\kappa_3 & 0 \\ 0 & 0 & \tau & -\kappa_4 \end{pmatrix} \tag{23}$$

is an upper bound of $A_{22}(x)$. For condition 5 of Theorem 4.2, we present the condition for a Metzler matrix $M$ to satisfy $\alpha(M) < 0$ using Lemma 4.3

**Lemma 4.3.** *Let $M(x)$be a Metzler matrix which is block decomposed as:*

$$M = \begin{pmatrix} \mathbb{A} & \mathbb{B} \\ \mathbb{C} & \mathbb{D} \end{pmatrix}, \tag{24}$$

*where $\mathbb{A}$ and $\mathbb{D}$ are square matrices. Then, M is Metzler stable if and only if $\mathbb{A}$ and $\mathbb{D} - \mathbb{C}^{-1}\mathbb{B}$ are Metzler stable.*

$$\mathbb{D}-\mathbb{C}^{-1}\mathbb{B}=\begin{bmatrix} \dfrac{-k_1k_3(k_2+\phi)(\mu+\alpha+\rho)+A_1\gamma\left[k_3(1-\theta)+\eta(k_2\theta+\phi)\right]}{k_1k_2(\mu+\alpha+\rho)-A_1\gamma(1-\theta)} & \dfrac{A_1\gamma\epsilon\left[(\phi(1-\theta)+k_2\theta)\right]-k_1(k_2+\phi)k_3(\mu+\alpha+\rho)}{k_1(k_2+\phi)(\mu+\alpha+\rho)-A_1\gamma(1-\theta)} \\ \tau & -\kappa_4 \end{bmatrix}$$

**Box II.**

In this case, $\bar{A}_{22}(x)$ is decomposed as:

$$A=\begin{pmatrix} -\kappa_1 & \dfrac{A_1}{\mu+\alpha+\rho} \\ (1-\theta)\gamma & -\kappa_2-\phi \end{pmatrix}, \qquad C=\begin{pmatrix} \theta\gamma & \phi \\ 0 & 0 \end{pmatrix}$$
$$B=\begin{pmatrix} \dfrac{A_1\eta}{\mu+\alpha+\rho} & \dfrac{A_1\epsilon}{\mu+\alpha+\rho} \\ 0 & 0 \end{pmatrix}, \qquad D=\begin{pmatrix} -\kappa_3 & 0 \\ \tau & -\kappa_4 \end{pmatrix} \tag{25}$$

and equation given in Box II. Therefore $\mathbb{D}-\mathbb{C}^{-1}\mathbb{B}$ is a Metzler matrix if $(\mathcal{R}_a,\mathcal{R}_s)<1$ in (26)

$$\begin{aligned}&\frac{-k_1k_3(k_2+\phi)(\mu+\alpha+\rho)+A_1\gamma\left[k_3(1-\theta)+\eta(k_2\theta+\phi)\right]}{k_1k_2(\mu+\alpha+\rho)-A_1\gamma(1-\theta)}\\ &=\frac{-k_1k_3(k_2+\phi)(\mu+\alpha+\rho)\left[1-(\mathcal{R}_a)+(1-\mathcal{R}_s)\right]}{k_1(k_2+\phi)(\mu+\alpha+\rho)(1-\mathcal{R}_a)}<1,\end{aligned} \tag{26}$$

and it is stable if

$$\begin{aligned}&\frac{k_1k_3k_4(k_2+\phi)(\mu+\alpha+\rho)-A_1\gamma\left[k_3k_4(1-\theta)+k_4\eta(k_2\theta+\phi)+\tau\epsilon(k_2\theta+\phi)\right]}{\kappa_1\kappa_2(\mu+\alpha+\rho)-A_1\gamma(1-\theta)}\\ &=\frac{k_1k_3k_4(k_2+\phi)(\mu+\alpha+\rho)(1-\mathcal{R}_{0V})}{ki(k_2+\phi)(\mu+\alpha+\rho)(1-\mathcal{R}_a)}=\frac{k_3\kappa_4(1-\mathcal{R}_{0V})}{(1-\mathcal{R}_a)}>0\end{aligned} \tag{27}$$

It should be noted that, condition (27) is a generalization of condition (26).

$$\text{Hence,}\qquad \mathcal{R}_{0V}<\frac{\gamma\beta\left[k_3k_4(1-\theta)+k_4\eta(k_2\theta+\phi)+\tau\epsilon(k_2\theta+\phi)\right]}{k_1k_3k_4(k_2+\phi)}<1 \tag{28}$$

Thus, satisfying condition (27) is sufficient for the GAS of the DFE. □

### 4.3. Endemic equilibrium ($\mathcal{E}_1$)

In order to establish the existence of endemic equilibria of model (2) (i.e, a scenario where at least one of the infected state variable of the model is non-zero), the model system (2) is solved in term of force of infection expressed as:

$$X^{**}=\frac{(I_a^{**}+\eta I_s^{**}+\epsilon H^{**})}{N^{**}} \tag{29}$$

We solve the equations of the model (2) at state variable in term of $X^{**}$ and we obtain:

$$\begin{aligned}
S^{**}&=\frac{k_1(k_2+\phi)(X^{**}\sigma+\alpha+\mu)I_a{}^{**}}{(1-\theta)\gamma X^{**}\left[(X^{**}\sigma+\alpha+\mu)\beta+(\rho\sigma)\right]}, \qquad H^{**}=\frac{\tau(k_2\theta+\phi)I_a^{**}}{k_3(1-\theta)K_4},\\
V^{**}&=\frac{k_1\rho(k_2+\phi)I_a^{**}}{(1-\theta)\gamma X^{**}\left[(X^{**}\sigma+\alpha+\mu)\beta+(\rho\sigma)\right]}, I_s^{**}=\frac{(k_2\theta+\phi)I_a^{**}}{k_3(1-\theta)}, E^{**}=\frac{I_a^{**}(k_2+\phi)}{(1-\theta)\gamma},\\
R^{**}&=\frac{\left\{\beta\sigma\left[(k_2+\phi)k_1I_a^{**}-\gamma\Lambda(1-\theta)\right]X^{**2}+(k_2+\phi)\left[\beta(\mu+\alpha)+\sigma(\mu+\rho)\right]k_1I_a^{**}X^{**}\right.}{\left.+\Lambda\gamma(1-\theta)\left[\beta(\mu+\alpha)+\rho\sigma\right]X^{**}+k_1(k_2+\phi)(\alpha+\mu+\rho)\mu I_a^{**}\right\}}\\
&\quad\gamma m(1-\theta)\left[X^{**}\beta\sigma+(\mu+\alpha)\beta+\rho\sigma\right]X^{**}\\
I_s^{**}&=\frac{\gamma(\mu+m)k_3(1-\theta)\Lambda k_4\left[(X^{**}\sigma+\alpha+\mu)\beta+\rho\sigma\right]X^{**}}{\left[k_1k_3k_4\beta\sigma\left[(k_2+\phi)(m+\mu)-\gamma(1-\theta)m\right]-\gamma m\beta\sigma\left[k_3\tau+k_2k_4\right](k_2\theta+\phi)\right]X^{**2}},\\
&\quad+\left\{\left(\left[(k_2+\phi)(\beta+\sigma)-\gamma\beta(1-\theta)\right]\mu+\left[k_2+\phi-\gamma(1-\theta)\right](\alpha\beta+\rho\sigma)\right)mk_1k_3k_4+\right.\\
&\quad\left.\mu(k_2+\phi)\left[\mu(\sigma+\beta)+\alpha\beta+\sigma\rho\right]-\gamma m(k_2\theta+\phi)\left[\alpha\beta+\beta\mu+\rho\sigma\right](k_3\tau+k_2k_4)\right\}X^{**}\\
&\quad+\mu k_1k_3k_4(\mu+m)\left[\alpha+\mu+\rho\right](k_2+\phi).
\end{aligned}$$

Substituting $\left(S^{**},\ V^{**},\ E^{**},\ I_a^{**},\ I_s^{**},H^{**},\ R^{**}\right)$ into (29) which gives

$$\begin{aligned}X^{**}=&\frac{(\mu+m)\gamma\beta\sigma T_1X^{**2}+(\mu+m)\gamma A_1T_1X^{**}}{\sigma\beta X^{**2}\left[T_2k_3\gamma+T_3\gamma+T_4k_3+\gamma\tau T_5\right]+k_3T_4k_1(\mu+\alpha+\rho)}\\ &+\left[T_2k_3+T_3\gamma A_1+T_4k_3A_1+\sigma T_4k_1k_3+\tau\gamma T_5A_1\right]X^{**},\end{aligned} \tag{30}$$

where

$$\begin{aligned}T_1&=\left[k_3k_4(1-\theta)+\eta k_4(k_2\theta+\phi)+\tau\epsilon(k_2\theta+\phi)\right],\\ T_2&=(k_1+m+\mu)(1-\theta)k_4,\\ T_3&=(k_2+m+\mu)(k_2\theta+\phi)k_4, \qquad T_4=(m+\mu)(k_2\theta+\phi)k_4,\\ T_5&=(k_3+m+\mu)(k_2\theta+\phi).\end{aligned}$$

Eq. (30) can be express as

$$\begin{aligned}X^{**}\left\{\sigma\beta X^{**2}\left[T_2k_3\gamma+T_3\gamma+T_4k_3+\gamma\tau T_5\right]+\left[T_2k_3+T_3\gamma A_1+T_4k_3A_1+\sigma T_4k_1k_3+\right.\right.\\ \left.\left.\tau\gamma T_5A_1-(\mu+m)\beta\gamma\sigma T_1\right]X^{**}+k_3k_1T_4(\mu+\alpha+\rho)-(\mu+m)\gamma A_1T_1\right\}=0.\end{aligned} \tag{31}$$

Moreover, equation from (31) $X^{**}=0$ or

$$\begin{aligned}\sigma\beta\left[T_2k_3\gamma+T_3\gamma+T_4k_3+\gamma\tau T_5\right]X^{**2}+\left[T_2k_3+T_3\gamma A_1+T_4k_3A_1+\sigma T_4k_1k_3+\right.\\ \left.\tau\gamma T_5A_1-(\mu+m)\beta\gamma\sigma T_1\right]X^{**}+k_3k_1T_4(\mu+\alpha+\rho)-(\mu+m)\gamma A_1T_1=0.\end{aligned} \tag{32}$$

Thus, from Eq. (32), we obtain the quadratic equation below:

$$a_2X^{**2}+a_1X^{**}+a_0=0, \tag{33}$$

with the coefficient of $X^{**}$ given as:

$$\begin{aligned}a_2&=\sigma\beta\left[T_2k_3\gamma+T_3\gamma+T_4k_3+\gamma\tau T_5\right],\\ a_1&=T_2k_3+T_3\gamma A_1+T_4k_3A_1+\sigma T_4k_1k_3+\tau\gamma T_5A_1-(\mu+m)\beta\gamma\sigma T_1,\\ a_0&=k_3k_4k_1(\mu+m)(k_2\theta+\phi)(\mu+\alpha+\rho)\left[1-\mathcal{R}_{0V}.\right]\end{aligned} \tag{34}$$

However, it is clear from Eq. (34) that $a_2$ is always positive and $a_0$ is negative whenever $\mathcal{R}_{0V}>1$. Hence, Theorem 4.4 summarizes the condition for existence of endemic equilibrium for the COVID-19 model (2).

**Theorem 4.4.** *The COVID-19 model (2) has:*

1. *no endemic equilibrium otherwise, if all the coefficient $\{a_2,\ a_1,\ a_0\}$ of Eq. (33) are all positive*
2. *a unique endemic equilibrium exists if $a_1<0$, and $a_0=0$ or ${a_1}^2-4a_0a_2=0$*
3. *two endemic equilibria if $a_0>0$, $a_1<0$ and ${a_1}^2-4a_0a_2>0$*
4. *a unique endemic equilibrium if $a_0<0\Leftrightarrow\mathcal{R}_{0V}>1$*

Thus, it is clear from Theorem 4.4 case (2) that the model system (2) has a unique endemic equilibrium whenever $\mathcal{R}_{0V}>1$. Furthermore, case (3) of Theorem 4.4 establishes the existence of multiple equilibrium points which indicates the possibility of backward bifurcation (where the locally-asymptotically stable DFE co-exists with a locally-asymptotically stable endemic equilibrium in the model(2) whenever $\mathcal{R}_{0V}<1$ (see, for instance, [6]). Hence, to compute the bifurcation, the discriminant of (33) is equated to zero. Thus,

$$\begin{aligned}\triangle=&{a_1}^2-4a_2k_3k_4k_1(\mu+m)(k_2+\phi)(\mu+\alpha+\rho)\left[1-\mathcal{R}_{0V}\right]=0\\ \mathcal{R}_{0V}^*=&1-\frac{{a_1}^2}{4a_2k_3k_4k_1(\mu+m)(k_2+\phi)(\mu+\alpha+\rho)}\end{aligned} \tag{35}$$

Therefore, Eq. (35) gives the analytical expression of a threshold value for the control reproduction number, and backward bifurcation would occur for values of $\mathcal{R}_{0V}^*<\mathcal{R}_{0v}<1$.

### 4.4. Backward bifurcation analysis

Over the years, it has been widely accepted that the condition $\mathcal{R}_0<1$ is sufficient for the elimination of a disease. However, this

standpoint has been challenged with a number of theoretical studies demonstrating that the criterion may not always be sufficient. Instead, the phenomenon of backward bifurcation offers a different interpretation since it shows that sometimes whenever $\mathcal{R}_0 < 1$ and the Disease Free Equilibrium is stable, there might still be another stable endemic equilibrium coexisting simultaneously. Thus, even if $\mathcal{R}_0 < 1$, a population may still tend toward an endemic equilibrium in which the disease persists indefinitely. This is the case when there are multiple stable equilibria coexisting simultaneously. In such scenarios, the eventual equilibrium a population will converge towards depends on the initial conditions (in terms of numbers of individuals) of its various sub-populations. Therefore, it is of great importance to indicate the type of bifurcation the model would exhibits under the influence of implemented control measures. Hence, we claim the following result.

**Theorem 4.5.**

$$Let \quad \rho^* = \frac{(\beta^* - \sigma)w_2 + \beta^*(\alpha+\mu)(w_1+w_4+w_5+w_6+w_7)}{(\beta^*-\sigma)w_1 - \sigma(w_1+w_4+w_5+w_6+w_7)} \tag{36}$$

*Then, at $\mathcal{R}_{0V} = 1$, model system (2) exhibits transcritical bifurcation and its direction is backward (or forward) iff $\rho^* < \rho$ (or $> \rho$).*

**Proof.** Suppose

$$\mathcal{E}_1 = \left(S^{**}, V^{**}, E^{**}, I_a^{**}, I_s^{**}, H^{**}, R^{**}\right) \tag{37}$$

represents any arbitrary endemic equilibrium of the model (2) (that is, an equilibrium in which at least one of the infected components is non-zero). Applying the Center Manifold theory [57], the existence of backward bifurcation will be studied. By simplification and change of variables of model (2). *Let* $S = x_1$, $V = x_2$, $E = x_3$, $I_a = x_4$, $I_s = x_5$, $H = x_6$, and $R = x_7$, *so that* $N = x_1+x_2+x_3+x_4+x_5+x_6+x_7$. Further, by using the vector notation $X = (x_1, x_2, x_3, x_4, x_5, x_6, x_7)^T$, the model (2) can be written in the form $\frac{dX}{dt} = F(X)$, with $(f_1, f_2, f_3, f_4, f_5, f_6, f_7,)^T$, as follows:

$$\begin{aligned}
\frac{dx_1}{dt} &\equiv f_1 = \Lambda + mx_7 + \alpha x_3 - \beta\kappa x_1 - (\mu+\rho)x_1\\
\frac{dx_2}{dt} &\equiv f_2 = \rho x_1 - \sigma\kappa x_2 - (\mu+\alpha)x_2\\
\frac{dx_3}{dt} &\equiv f_3 = \beta\kappa x_1 + \sigma\kappa x_2 - (\gamma+\mu)x_3\\
\frac{dx_4}{dt} &\equiv f_4 = (1-\theta)\gamma x_3 - (\psi_1+\phi+\mu)x_4\\
\frac{dx_5}{dt} &\equiv f_5 = \theta\gamma x_3 + \phi x_4 - (\psi_2+\tau+\delta_1+\mu)x_5\\
\frac{dx_6}{dt} &\equiv f_6 = \tau x_5 - (\psi_3+\delta_2+\mu)x_6\\
\frac{dx_7}{dt} &\equiv f_7 = \psi_1 x_4 + \psi_2 x_5 + \psi_3 x_6 - (\mu+m)x_7
\end{aligned} \tag{38}$$

The force of infection is given as

$$\kappa = \frac{(x_4 + \eta x_5 + \epsilon x_6)}{x_1+x_2+x_3+x_4+x_5+x_6+x_7},$$
$$\beta = \beta_1(1-w-s) \text{ and } \sigma = \sigma_1(1-w-s)$$

Considering the case when $\mathcal{R}_{0V} = 1$ and that $\beta = \beta^*$ is chosen as a bifurcation parameter. Solving for $\beta = \beta^*$ in (14) gives

$$1 = \frac{\gamma\left[\beta(\mu+\alpha)+\rho\sigma\right]\left[k_3k_4(1-\theta)+k_4\eta(k_2\theta+\phi)+\tau\epsilon(k_2\theta+\phi)\right]}{k_1k_3k_4(\mu+\alpha+\rho)(k_2\theta+\phi)} \tag{39}$$

$$\beta^* = \frac{(\mu+\alpha+\rho)(k_2+\phi)k_1k_3k_4 - \rho\sigma\gamma T_1}{\gamma(\mu+\alpha)T_1} \tag{40}$$

The Jacobian for the transformed model (2) at the DFE ($\mathcal{E}_0$) with $\beta = \beta^*$ is given as (41) in Box III.

The Jacobian $J^*(E_0)$ of the linearized model (38) has a simple zero eigenvalue (with all other eigenvalues having negative real part). Hence, the Center Manifold Theory [57] is used to analyze the dynamics of model (38). However, the right eigenvector ($w$) and left eigenvector ($v$) are computed from $J^*(E_0)_{|\beta=\beta*}$ given as:

$$\begin{aligned}
w_1 &= \frac{\gamma\left\{\left[(\mu+\alpha)(\mu+\alpha)[(\mu+m)\beta^*T_1 - Qm] + (\alpha\mu+m)\sigma\rho T_1 - Qm\rho(1+\mu)\right]\right\}}{\mu(\mu+\alpha+\rho)^2(k_2+\phi)k_3k_4}\\
w_2 &= \frac{\gamma\rho\left\{\mu(\mu+m)(\beta^*+\sigma)T_1 - m(\mu+\alpha+\rho)Q\right\}}{\mu(\mu+\alpha+\rho)^2(k_2+\phi)k_3k_4},\ w_3 = 1,\ w_4 = \frac{\gamma(1-\theta)}{k_2+\phi},\\
w_5 &= \frac{\gamma(k_2\theta+\phi)}{k_3(k_2+\phi)},\ w_6 = \frac{\gamma\tau(k_2\theta+\phi)}{k_3k_4(k_2+\phi)},\ w_7 = \frac{\gamma Q}{k_3k_4(k_2+\phi)(\mu+m)}
\end{aligned}$$

With $Q$ define as $(k_2\theta+\phi)[k_4\psi_2+\tau\psi_3] + k_3\psi_1(1-\theta)$ and we compute a left eigenvector satisfying v.w = 1 given by

$$\begin{aligned}
v_1 &= 0,\ v_2 = 0,\ v_3 = 1,\ v_4 = \frac{k_1k_2k_3(\mu+\alpha+\rho) - A_1\gamma\theta(\eta k_4 - \epsilon\tau)}{k_3k_4(\mu+\alpha+\rho)(1-\theta)\gamma},\\
v_5 &= \frac{A_1(\epsilon\tau+\eta k_4)}{k_3k_4(\mu+\alpha+\rho)},\ v_6 = \frac{A_1\epsilon}{k_4(\mu+\alpha+\rho)},\ v_7 = 0
\end{aligned} \tag{42}$$

Furthermore, the associated non zero second partial derivatives of model (38) evaluated at $(E_0, \beta^*)$ is obtained as:

$$\begin{aligned}
\frac{\partial f_3}{\partial x_1\partial x_4} &= \frac{\partial f_3}{\partial x_4\partial x_1} = \frac{\mu\rho(\beta-\sigma)}{\Lambda(\mu+\alpha+\rho)},\\
\frac{\partial f_3}{\partial x_1\partial x_5} &= \frac{\partial f_3}{\partial x_5\partial x_1} = \frac{\mu\rho(\beta-\sigma)\eta}{\Lambda(\mu+\alpha+\rho)},\\
\frac{\partial f_3}{\partial x_1\partial x_6} &= \frac{\partial f_3}{\partial x_6\partial x_1} = \frac{\mu\rho(\beta-\sigma)\epsilon}{\Lambda(\mu+\alpha+\rho)},\\
\frac{\partial f_3}{\partial x_2\partial x_4} &= \frac{\partial f_3}{\partial x_4\partial x_2} = \frac{-\mu\rho(\beta-\sigma)(\mu+\alpha)}{\Lambda(\mu+\alpha+\rho)}\\
\frac{\partial f_3}{\partial x_2\partial x_5} &= \frac{\partial f_3}{\partial x_5\partial x_2} = \frac{-\mu\rho(\beta-\sigma)(\mu+\alpha)\eta}{\Lambda(\mu+\alpha+\rho)},\\
\frac{\partial f_3}{\partial x_2\partial x_6} &= \frac{\partial f_3}{\partial x_6\partial x_2} = \frac{-\mu\rho(\beta-\sigma)(\mu+\alpha)\epsilon}{\Lambda(\mu+\alpha+\rho)}\\
\frac{\partial f_3}{\partial x_3\partial x_4} &= \frac{\partial f_3}{\partial x_4\partial x_3} = \frac{-\mu\left[\beta(\mu+\alpha)+\sigma\rho\right]}{\Lambda(\mu+\alpha+\rho)},\\
\frac{\partial f_3}{\partial x_3\partial x_5} &= \frac{\partial f_3}{\partial x_5\partial x_3} = \frac{-\mu\left[\beta(\mu+\alpha)+\sigma\rho\right]\eta}{\Lambda(\mu+\alpha+\rho)}\\
\frac{\partial f_3}{\partial x_3\partial x_6} &= \frac{\partial f_3}{\partial x_6\partial x_3} = \frac{-\mu\left[\beta(\mu+\alpha)+\sigma\rho\right]\epsilon}{\Lambda(\mu+\alpha+\rho)},\\
\frac{\partial f_3}{\partial x_4\partial x_4} &= -2\frac{\mu\left[\beta(\mu+\alpha)+\sigma\rho\right]}{\Lambda(\mu+\alpha+\rho)}\\
\frac{\partial f_3}{\partial x_4\partial x_5} &= \frac{\partial f_3}{\partial x_5\partial x_4} = \frac{-\mu(\eta+1)\left[\beta(\mu+\alpha)+\sigma\rho\right]}{\Lambda(\mu+\alpha+\rho)},\\
\frac{\partial f_3}{\partial x_4\partial x_6} &= \frac{\partial f_3}{\partial x_6\partial x_4} = \frac{-\mu(\epsilon+1)\left[\beta(\mu+\alpha)+\sigma\rho\right]}{\Lambda(\mu+\alpha+\rho)}\\
\frac{\partial f_3}{\partial x_4\partial x_7} &= \frac{\partial f_3}{\partial x_7\partial x_4} = \frac{-\mu\left[\beta(\mu+\alpha)+\sigma\rho\right]\epsilon}{\Lambda(\mu+\alpha+\rho)},\\
\frac{\partial f_3}{\partial x_5\partial x_5} &= -2\frac{\mu\left[\beta(\mu+\alpha)+\sigma\rho\right]\eta}{\Lambda(\mu+\alpha+\rho)}\\
\frac{\partial f_3}{\partial x_5\partial x_6} &= \frac{\partial f_3}{\partial x_6\partial x_5} = \frac{-\mu(\eta+\epsilon)\left[\beta(\mu+\alpha)+\sigma\rho\right]}{\Lambda(\mu+\alpha+\rho)}\\
\frac{\partial f_3}{\partial x_5\partial x_7} &= \frac{\partial f_3}{\partial x_7\partial x_5} = \frac{-\mu\left[\beta(\mu+\alpha)+\sigma\rho\right]\eta}{\Lambda(\mu+\alpha+\rho)}\\
\frac{\partial f_3}{\partial x_6\partial x_6} &= \frac{\partial f_3}{\partial x_6\partial x_6} = -2\frac{\mu\left[\beta(\mu+\alpha)+\sigma\rho\right]\eta}{\Lambda(\mu+\alpha+\rho)}
\end{aligned}$$

Now, the coefficient of $\bar{a}$ and $\bar{b}$ defined by Theorem 4.5 in [57] is calculated as follows:

$$\begin{aligned}
\bar{b} &= \sum_{k,i,=1}^{7} v_k w_i \frac{\partial^2 f_k}{\partial x_i\partial\beta}(E_0, 0)\\
&= v_1w_4\frac{\partial^2 f_1}{\partial x_1\partial\beta} + v_1w_5\frac{\partial^2 f_1}{\partial x_5\partial\beta} + v_1w_6\frac{\partial^2 f_1}{\partial x_6\partial\beta}\\
&\quad + v_3w_4\frac{\partial^2 f_3}{\partial x_4\partial\beta} + v_3w_5\frac{\partial^2 f_3}{\partial x_5\partial\beta} + v_3w_6\frac{\partial^2 f_3}{\partial x_6\partial\beta}\\
&= 0 + 0 + 0 + \frac{\gamma(1-\theta)(\mu+\alpha)}{(k_2+\phi)(\mu+\alpha+\rho)} + \frac{\gamma\eta(k_2\theta+\phi)(\mu+\alpha)}{k_3(k_2+\phi)(\mu+\alpha+\rho)}\\
&\quad + \frac{\gamma\epsilon\tau(k_2\theta+\phi)(\mu+\alpha)}{k_3k_4(k_2+\phi)(\mu+\alpha+\rho)}\\
&= \frac{\gamma(\mu+\alpha)[k_3k_4(1-\theta) + (k_4\eta+\epsilon\tau)(k_2\theta+\phi)]}{(k_2+\phi)(\mu+\alpha+\rho)k_3k_4}\\
&= \frac{\gamma(\mu+\alpha)T_1}{(k_2+\phi)(\mu+\alpha+\rho)k_3k_4} > 0
\end{aligned} \tag{43}$$

$$J^*(E_0)=\begin{bmatrix} -(\mu+\rho) & \alpha & 0 & -\frac{\beta^*(\mu+\alpha)}{\mu+\alpha+\rho} & -\frac{\eta\beta^*(\mu+\alpha)}{\mu+\alpha+\rho} & -\frac{\epsilon\beta^*(\mu+\alpha)}{\mu+\alpha+\rho} & m \\ \rho & -(\alpha+\mu) & 0 & -\frac{\sigma\rho}{\mu+\alpha+\rho} & \frac{-\eta\sigma\rho}{\mu+\alpha+\rho} & -\frac{\epsilon\sigma\rho}{\mu+\alpha+\rho} & 0 \\ 0 & 0 & \kappa_1 & \frac{\beta^*(\mu+\alpha)+\sigma_1\rho}{\mu+\alpha+\rho} & \frac{\eta\left[\beta^*(\mu+\alpha)+\sigma_1\rho\right]}{\mu+\alpha+\rho} & \frac{\epsilon\left[\beta^*(\mu+\alpha)+\sigma_1\rho\right]}{\mu+\alpha+\rho} & 0 \\ 0 & 0 & (1-\theta)\gamma & -\kappa_2 & 0 & 0 & 0 \\ 0 & 0 & \theta\gamma & \phi & -\kappa_3 & 0 & 0 \\ 0 & 0 & 0 & 0 & \tau & -\kappa_4 & 0 \\ 0 & 0 & 0 & \psi_1 & \psi_2 & \psi_3 & -(\mu+m) \end{bmatrix} \tag{41}$$

**Box III.**

$$\begin{aligned}\bar{a}=&\sum_{k,i,j,=1}^{7} v_k w_i w_j \frac{\partial^2 f_k}{\partial x_i \partial \beta}(E_0,\beta^*)\\ =&v_3w_1\left[w_4\frac{\partial f_3}{\partial x_1\partial x_4}+w_5\frac{\partial f_3}{\partial x_1\partial x_5}+w_6\frac{\partial f_3}{\partial x_1\partial x_6}\right]\\ &+v_3w_2\left[w_4\frac{\partial f_3}{\partial x_2\partial x_4}+w_5\frac{\partial f_3}{\partial x_2\partial x_5}+w_6\frac{\partial f_3}{\partial x_2\partial x_6}\right]\\ &+v_3w_4\left[w_1\frac{\partial f_3}{\partial x_4\partial x_1}+w_2\frac{\partial f_3}{\partial x_4\partial x_2}+w_3\frac{\partial f_3}{\partial x_4\partial x_3}+w_4\frac{\partial f_3}{\partial x_4\partial x_4}\right.\\ &\left.+w_5\frac{\partial f_3}{\partial x_4\partial x_5}+w_6\frac{\partial f_3}{\partial x_4\partial x_6}+w_7\frac{\partial f_3}{\partial x_4\partial x_7}\right]\\ &+v_3w_5\left[w_1\frac{\partial f_3}{\partial x_5\partial x_1}+w_2\frac{\partial f_3}{\partial x_5\partial x_2}+w_3\frac{\partial f_3}{\partial x_5\partial x_3}+w_4\frac{\partial f_3}{\partial x_5\partial x_4}\right.\\ &\left.+w_5\frac{\partial f_3}{\partial x_5\partial x_5}+w_6\frac{\partial f_3}{\partial x_5\partial x_6}+w_7\frac{\partial f_3}{\partial x_5\partial x_7}\right]\\ &+v_3w_6\left[w_1\frac{\partial f_3}{\partial x_6\partial x_1}+w_2\frac{\partial f_3}{\partial x_6\partial x_2}+w_3\frac{\partial f_3}{\partial x_6\partial x_3}+w_4\frac{\partial f_3}{\partial x_6\partial x_4}\right.\\ &\left.+w_5\frac{\partial f_3}{\partial x_6\partial x_5}+w_6\frac{\partial f_3}{\partial x_6\partial x_6}+w_7\frac{\partial f_3}{\partial x_6\partial x_7}\right]\\ &+v_3w_3\left[w_4\frac{\partial f_3}{\partial x_3\partial x_4}+w_5\frac{\partial f_3}{\partial x_3\partial x_5}+w_6\frac{\partial f_3}{\partial x_3\partial x_6}\right]\\ &+v_3w_7\left[w_4\frac{\partial f_3}{\partial x_7\partial x_4}+w_5\frac{\partial f_3}{\partial x_7\partial x_5}+w_6\frac{\partial f_3}{\partial x_7\partial x_6}\right]\end{aligned}$$

$$\bar{a}=\frac{2\mu(\beta^*-\sigma)\gamma T_1\left[w_1\rho-w_2\right]-2\mu\left[\beta^*(\mu+\alpha)+\sigma\rho\right]\gamma T_1\left[w_1+w_4+w_5+w_6+w_7\right]}{\Lambda(\mu+\alpha+\rho)k_3k_4(k_2+\phi)} \tag{44}$$

Based on the computed coefficient of $\bar{a}$ and $\bar{b}$, it is clear that coefficient $\bar{b}$ defined in Eq. (43) is always positive. Therefore, model system (38) will undergoes backward bifurcation at $\mathcal{R}_{0V}=1$, if $\bar{a}>0$, that is if $(\rho^*<\rho)$ as define on Eq. (36) and will undergo a forward bifurcation at $\mathcal{R}_{0V}=1$, if $\bar{a}<0$, that is if $(\rho^*>\rho)$, conclusively, this established Theorem 4.5. In other words, this study shows that the backward bifurcation property of model (38) arises when the rate of vaccination ($\rho$) is not large enough (Such that the fraction of vaccinated individual at the disease free equilibrium does not exceed the calculated value $\rho^*$) (see Fig. 3).

The condition of backward bifurcation clearly shows the importance of vaccination. For higher value of $\rho(>\rho^*)$, the condition $\mathcal{R}_{0V}<1$ is insufficient for eliminating coronavirus epidemic and a slight change in vaccination rate on population can alter the success of intervention. However, the presence of backward bifurcation in the transmission dynamics of COVID-19 disease make effective control or elimination difficult, since $\mathcal{R}_{0V}$ has to be significantly less than unity.

## 5. Parameter estimation and sensitivity analysis

In order to use the newly proposed epidemiological model to simulate COVID-19 disease scenario in Nigeria, and to access the impact of vaccination and other control strategies. It is crucial to validate and provide some measure of reliability of our proposed model. This is achieved by extracting available COVID-19 real data from NCDC and Our World in Data [11,18], which helps in fitting the model outputs to observed data and using the process to get best values for some unknown parameters which we do not have realistic estimate for. Thus, we adopts this approach via nonlinear least-squares curve fitting method by minimizing the sum of squares. In all, there are 20 biological parameters associated with the proposed model, some of the parameters $(\psi_1,\psi_2,\psi_3,\Lambda,\gamma)$ have been obtained from available literature, while the remaining parameters $(\alpha,m,\delta_1,\delta_2,\rho,\phi,\epsilon,\eta,\alpha,\beta_1,\sigma_1,s,w,\tau,\mu)$ are estimated using available information and referenced in Table 2

### 5.1. Baseline values of parameters for the model

The proposed Model (2) study the transmission dynamics of the dominant strain of Corona virus with impact of vaccination in Nigeria. To carry out the simulation, we used current outbreak data released and published daily by the Nigeria Center for Disease Control (NCDC) and Our World in Data [11,58] to extract data for define state variables and known parameters for our model fitting to obtain a good fit for the unknown parameters estimation. We carry out the model numerical simulations for an epidemic period starting from March 9, 2020 six days after the index case was detected in Nigeria to August 9 2020. Within these period partial lock-down with strict measures, social distancing and face mask usage were enforce in public). Based on information in [24] the incubation period for COVID-19 is estimated to average 5.1 days, with a range of 3 to 14 days. Thus, we set baseline value for $\gamma=1/5.1$. However, several studies [24,25] have assumed that transmission rate of asymptomatic infection was 0.5 times that of symptomatic infections, hence we set baseline value of $\theta=1/2$. Nevertheless, the fraction of infectious cases that are asymptomatic is uncertain. Moreover, the average recovery period for asymptomatic and symptomatic is about 7–15 days, so we set baseline value of $\psi_1,\psi_2=1/7$ and the hospitalized/self isolated recovery rate to $\psi_3=1/15$, while the recruitment into the susceptible population was estimated from [59] to a baseline value of $\Lambda=13942$ per day as at when the total population was 211,400,703. Furthermore, we adopt the initial number of infected individuals as at when the index case was reported from NCDC site and estimated the numbers of exposed individuals, since it is expected that some individuals might have been exposed within the population (since wide spread population screening and testing for COVID-19 had not begun at the time). Therefore, the initial conditions for the state variables of the model are chosen at $S(0)=211400691$, $V(0)=0$, $E(0)=11$, $I_A(0)=0$, $I_S(0)=2$, $H(0)=0$, $R(0)=0$ and the fitted parameters are presented in Table 2, while fitted curve is depicted in Fig. 4.

As displayed above, the real COVID-19 Nigerian cases and the fitted curve have been shown in Fig. 4(a) wherein it is observed that the model fits NCDC data well enough. Furthermore, Fig. 4(b) show a justified trend of the obtained residuals as they are scattered evenly below and above the horizontal line. By implication, residuals are useful for detecting outlying y-values and checking the linear regression

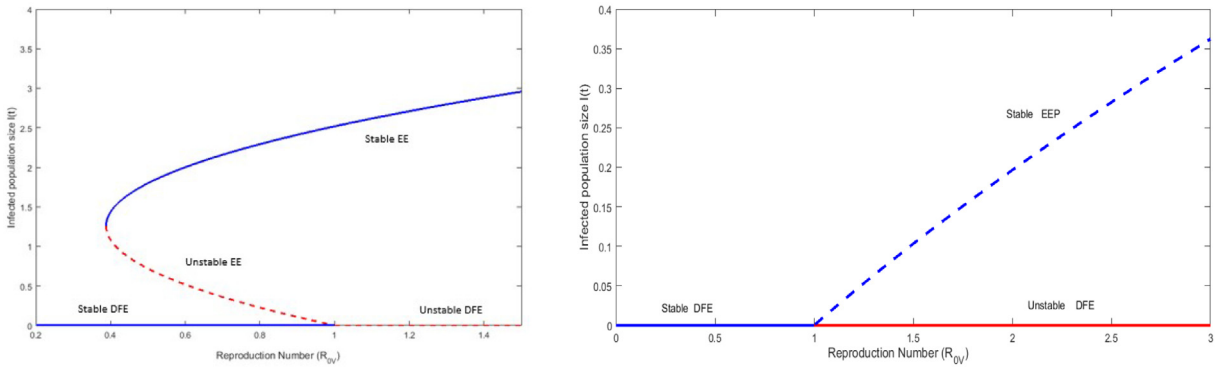


(a) Backward Bifurcation (b) Forward Bifurcation

**Fig. 3.** (a) Bifurcation diagram for backward bifurcation in the plane $(R_0, I^*)$, Parameter value use are $\gamma = 10, \delta_1 = 2.99e-1, \rho = 4$ and (b) Forward bifurcation in the plane $(R_0, I^*)$, Parameter value use are $\gamma = 7.15e-02, \delta_1 = 1.50e-2, \rho = 1.0795$ other parameters are presented in Table 2.

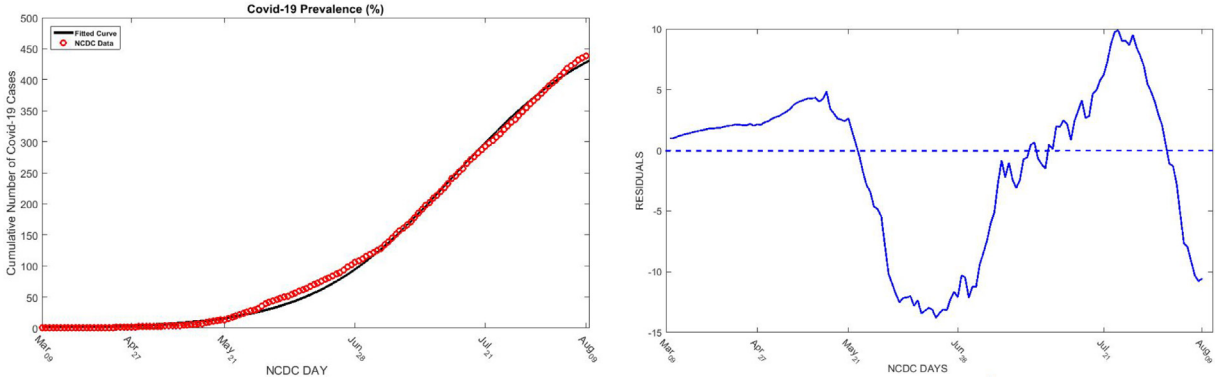


(a) Daily COVID-19 cumulative cases time series in Nigeria (b) Residuals for the best fitted curve

**Fig. 4.** (a) The daily COVID-19 cumulative cases time series in Nigeria from March 09 to August 09, 2020 with the best fitted curve from simulations of the proposed model and (b) the residuals for the best fitted curve.

assumptions with respect to the error term in the regression model. High-leverage observations have smaller residuals because they often shift the regression line or surface closer to them (i.e The numbers for residues show the vertical distance between reported data and fitted curve). Thus, when such residues are observed to be scattered randomly above and below the horizontal line, then the fitting is justified as represented in Fig. 4.

### 5.2. Sensitivity analysis

This section investigates how a percentage change in the key parameters in the model affects the control reproduction number and reveals the significance of each parameters on the spread of coronavirus disease. Moreover, the sensitivity analysis equally exposes the relation between variability in the model predictions and uncertainty in the model parameter values. Here, the sensitivity analysis is carried out using Latin Hypercube Sampling/Partial Rank Correlation Coefficient (LHS/PRCC) which is a more robust form of sensitivity analysis for a multidimensional parameter space. We explore the dependence of the entire parameter space of the model using the control reproduction number ($\mathcal{R}_{0V}$) as the output function with a minimum number of computer simulation [56,60]. As an application of the LHS/PRCC sensitivity analysis theory, we explore the relationship between the control reproduction number ($\mathcal{R}_{0V}$) and the parameters constituting it by ranking the significance of each parameter. The LHS matrices was generated by assuming all the model parameters are uniformly distributed, the PRCC of the control reproduction number are computed with parameter ranges as presented in Table 2. and PRCC plot is depicted in Fig. 5.

**Table 2**
Baseline values of the parameters used in Model (2).

| Parameters from Literature | Values (Range) | unit | Reference (Source) |
|---|---|---|---|
| $\Lambda$ | 13942 | $day^{-1}$ | [5] |
| $\gamma$ | 7.15e−02 | $day^{-1}$ | [36] |
| $\psi_1$ | 1.429e−01 | $day^{-1}$ | [36] |
| $\psi_2$ | 1.429e−01 | $day^{-1}$ | [36] |
| $\psi_3$ | 7.14e−02 | $day^{-1}$ | [24] |
| $\theta$ | 5.000e−01 | $day^{-1}$ | [24] |
| **Fitted Parameter** | | | |
| $m$ | $1.002e-01$ (2.000 − 0.100) | $day^{-1}$ | Fitted |
| $\alpha$ | 2.1868 (3.000 − 0.0043) | $day^{-1}$ | Fitted |
| $\rho$ | 1.0795 (2.000 − 0.600) | $day^{-1}$ | Fitted |
| $\delta_1$ | $1.50e-02$ (5 − 0.0009) | $day^{-1}$ | Fitted |
| $\delta_2$ | $2.50e-02$ (5 − 0.0001) | $day^{-1}$ | Fitted |
| $\phi$ | 1.0000 (1 − 0.0345) | $day^{-1}$ | Fitted |
| $\tau$ | $3.43e-02$ (3 − 0.0343) | $day^{-1}$ | Fitted |
| $\sigma_1$ | 2.5625 (5 − 0.0529) | $day^{-1}$ | Fitted |
| $\beta_1$ | 2.5265 (5 − 0.00529) | $day^{-1}$ | Fitted |
| $w$ | $1.60e-03$ (0.9 − 0.0013) | $day^{-1}$ | Fitted |
| $s$ | $5.200e-01$ (1 − 0.0040) | $day^{-1}$ | Fitted |
| $\eta$ | $5.377e-01$ (1 − 0.0034) | $day^{-1}$ | Fitted |
| $\epsilon$ | $1.13e-01$ (0.9 − 0.0056) | $day^{-1}$ | Fitted |
| $\mu$ | $6.99e-01$ (0.7 − 0.0014) | $day^{-1}$ | Fitted |

Fig. 5 shows how the threshold quantity $\mathcal{R}_{0V}$ varies with respect to changes in each of the model parameters. It reveals that the parameters that have the most positive influence on the values of $\mathcal{R}_{0V}$ are the effective infection rate of susceptible individuals ($\beta$) which by definition drives the infection in the entire population, the progression

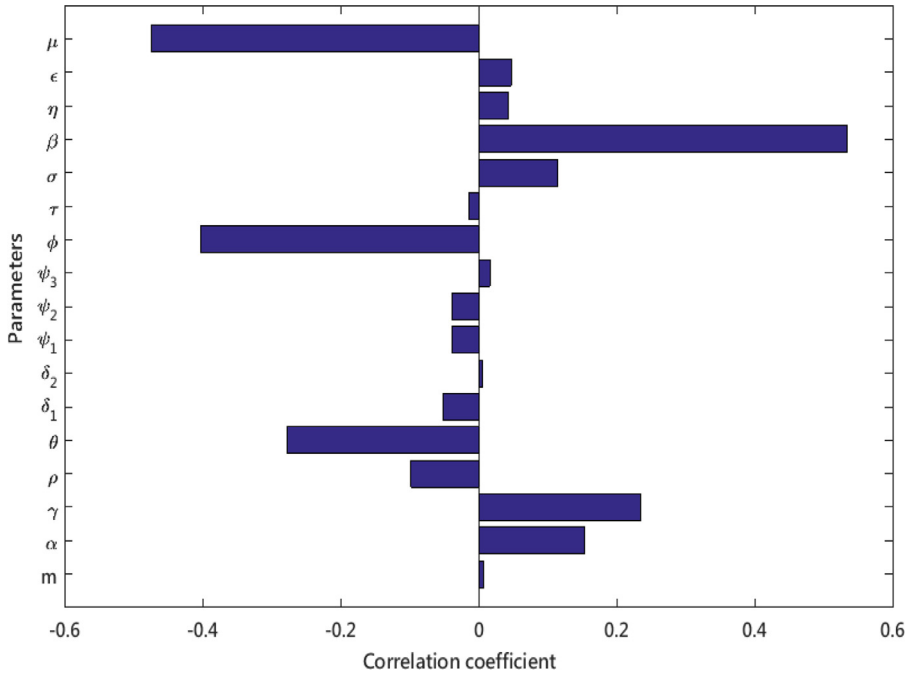


**Fig. 5.** Sensitivity plot of the reproduction number.

rate from exposed compartment ($\gamma$), the rate at which vaccinated individual losses their immunity ($\alpha$), and rate at which vaccinated individuals becomes infected ($\sigma$) while the parameter ($\mu$) has the most negative correlation to $\mathcal{R}_{0V}$ since natural death limit COVID-19 transmission. Moreover, $\psi$, $\theta$ and $\rho$ also have a negative correlation to $\mathcal{R}_{0V}$. Nevertheless, the implications of some of these sensitivity indices cannot be under-estimated. For example, the strong positive correlation of $\beta$ (infection rate) to $\mathcal{R}_{0V}$ implies that all measures that can limit individuals' contact with the virus would be effective in curtailing the spread of the disease. This indirectly implies that all the NPI measures should be sustained in order to continuously contain the pandemic. Also, the significant positive correlation of $\gamma$ (disease progression rate) to $\mathcal{R}_{0V}$ indicates that if individuals s can imbibe immune boosting nutrition which will attenuate the progression of Covid-19 exposed individuals into the infectious stages of the disease, then the spread of the disease would be indirectly reduced. In addition, the positive correlation of $\alpha$ (waning rate) to $\mathcal{R}_{0V}$ shows that improving the potency of the vaccine to ensure the vaccine-imposed immunity lasts relatively longer will help reduce the spread of the disease.

On the contrary, $\phi$ and $\theta$ negative correlation to $\mathcal{R}_{0V}$ shows that immune levels of the infected individuals will also determine how quickly infected individuals move into the symptomatically infectious compartment. Thus, corroborating the fact that immune boosting nutrition and impact of previous vaccination before or during infection could slow down the progression of the disease towards severity while equally facilitating quick recovery. In general, the results from the sensitivity analysis with respect to each of the other remaining model parameters can be similarly discussed.

## 6. Simulation results and discussions

In this section, we investigate the dynamics of the proposed model Eqs. (2) numerically for different sets of parameter values, by considering two different scenarios: first prior to introduction of vaccines and secondly during the vaccination administration era in order to elucidate the impact of vaccination on the spread of Covid-19 dominant strain. The motive is to examine the impact of varying different sensitive parameters values and also to support obtained theoretical results. Nevertheless, the hypothetical values of parameters given in Table 2 are found to be biologically feasible. Thus, we performed the numerical simulation using Runge–Kutta fourth order scheme for solving non-stiff system of ordinary differential equations with chosen initial conditions and estimated parameters as presented in Table 2.

Scenario 1: Evolution of each sub-population prior to introduction of vaccine; this was successfully carried out by setting the vaccinated population compartment of the model to zero ($V = 0$) and vaccination rate ($\rho = 0$) which ensures conformity to NCDC data. The observe behavior for each sub population (1.e Infected, Hospitalized and Recovery individuals), keeping in mind that precautionary measures such as wearing of face mask, regular personal hygiene and observing social distancing in public places were the mitigating measures to fight against Covid-19 from the onset of the outbreak until November 2020.

As represented in Fig. 6, we examine the evolution of the sub population without vaccination while considering the case when the basic reproduction is less than unity or greater than unity to understand the dynamics of Covid-19 disease. In Fig. 6(a), there is a steady declined in the population of exposed, asymptomatic and symptomatic infected individuals when the force of infection ($\beta$) was reduced to 0.2124 yielding a basic reproduction of number $\mathcal{R}_0 = 0.8403$ which resulted from increasing precautionary measures of keeping social distancing ($s$) and wearing of face-mask ($\omega$) in public places. Furthermore, the number of recovered and hospitalized individuals increased gradually, reaching a peak until it steadily decline all through a period of three months. By implication, our simulation result would have predicted the Nigeria Covid-19 situation if Nigerian Government had enforced the use of precautionary measures such as social distancing and wearing of face mask to curb transmission of the disease at the start of the Covid-19 outbreak, but that was not the case until two month later when the Lagos state government declared the use of NPI mandatory in public places from 25th April 2020. Conversely, Fig. 6(b) reveals the ideal situation when the basic reproduction is greater than unity ($\mathcal{R}_0 = 2.47$) in absence of vaccination. The expose sub-population have a rapid increase with the effective contact rate ($\beta = 1.2087$) which within the first two months exposes about 4.5 million persons resulting in a steady growth of both symptomatic and asymptomatic infected individuals within three months until the population begins to attain stability thereafter which may be due to strengthening of non-pharmaceutical measures that was later imposed.

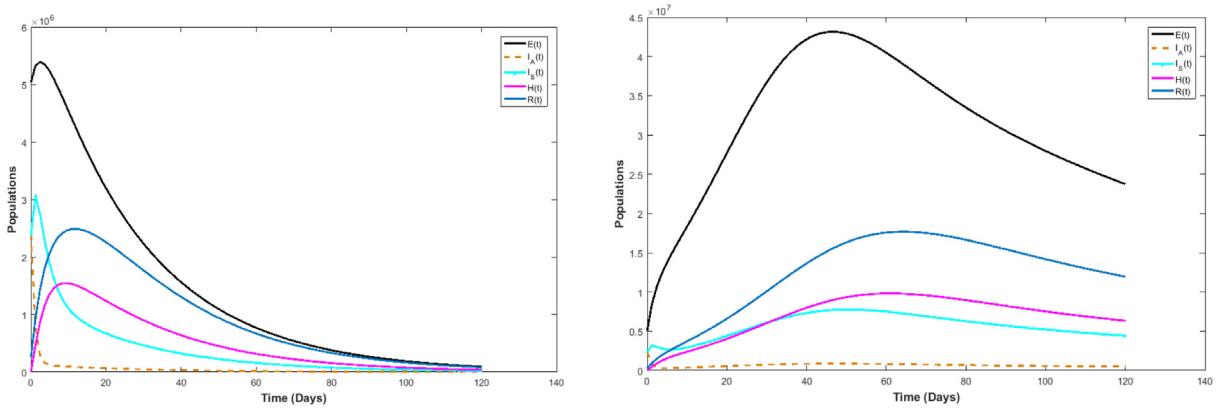


(a) Evolution of sub population when $\mathcal{R}_0 < 1$ (b) Evolution of sub population when $\mathcal{R}_0 > 1$

**Fig. 6.** (a) The Evolution of sub-population with time before introduction of vaccine when the basic reproduction number is less or greater than unity.

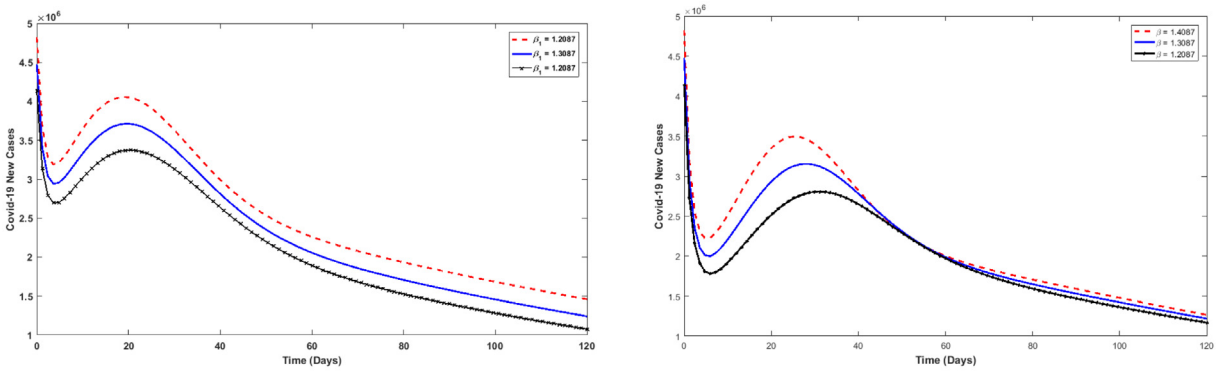


(a) Evolution of sub population at $\mathcal{R}_0 > 1$ when, $V \neq 0$ (b) Evolution of sub population at $\mathcal{R}_0 > 1$, when $V = 0$

**Fig. 7.** Assessment of the impact of different values of $\beta$ on new cases of Covid 19 in Nigeria The Evolution of sub-population with time prior to introduction of vaccine when the basic reproduction number is less or greater than unity.

Fig. 7 depicts the numerical simulation for new cases of Covid 19 disease in a time span of 120 days. while varying the force of infection ($\beta = 1.2087, 1.3087, 1.4087$) with and without vaccination when the basic reproduction is greater than unity. Fig. 7(a) reveals the impact of vaccination in curbing the spread of corona virus when compared with the dynamic behavior of new cases in 7(b) without vaccination. It can easily be observed from Fig. 7(a) when $\beta = 1.2018$ the population of new cases with vaccination sharply decrease within the first few days to 2.7 million, thereafter increase gradually due to indifference in perception about the vaccine within the first few month of vaccine introduction. However, after few days, as all government parastatal and private sectors begin to enforce vaccination, create public awareness and enlightenment on impact of vaccination to her citizens, the level of new cases begins to attain a downward trend until stationarity is achieved. Thus, similar trend was observed from the graph as we further increase the force of infection from $\beta = 1.2018$ *to* $\beta = 1.4018$.

Conversely, in Fig. 7(b) using the same set of parameters in Table 2, without considering sub-vaccination population, a drastic decrease in the number of new cases was established from 1.9 million to 1.7 million individuals which could be attributed to the use of non-pharmaceutical measures in mitigating the spread over time, but the impact was not as obvious to when vaccination was introduced to the sub population (comparing Figs. 7(a) and 7(b)). By implication, it reveals that in absence of vaccination about 70% of the population have to adheres strictly to the non-pharmaceutical intervention in order to achieve substantial reduction in numbers of new cases of Covid 19 (which is in conformity with Okuonghae assertion in [[25], section 4.3]) as compared to about 46% of the population which needs to be vaccinated in order to have substantial decrease of new cases of Corona virus in Nigeria.

Fig. 8 depicts the prevalence of Covid 19 in our model with and without vaccination. In Fig. 8(a), the solution profiles obtained show the worse peak rate of 2.4 million infected individuals nationwide if no vaccination was implemented along with adherence to preventive measures. However, the simulations were further carried out to assess the population-level impact of vaccination, by running the model (2) with various values of effective contact rate as represented in Fig. 8(b) and this reveal a significant decrease of 10% disease prevalence within the same time span. This implies that vaccination will play a significant role in combating Covid-19 nationwide. From the simulation, a peak prevalence of 1.8 million infected individuals was observed as compared with upward growth of 2.1 million infected individuals without vaccine administration and this possibly justify the reason for the relaxation of enforcement on the use of NPI's in public places after the introduction of vaccination.

In addition, the dynamics of infected individuals (asymptomatic and symptomatic) were simulated to investigate the impact of vaccination rate ($\rho$) and vaccine potency as a result of immunity loss ($\alpha$) on the disease dynamics. The results obtained with various vaccine efficacy ($\alpha = 0.2,\ 0.5,\ 1$), depicted in 9(a), show a marked decrease in the number of asymptomatic population (represented by solid lines) which continue to maintain its steady state, but a gradual increase of symptomatic individual (represented by dash line) was accounted for over time in the population as people migrate from being pre-symptomatic to symptomatic until it reaches a peak and gradually decline thereafter. This account for the impact of vaccination in slowing

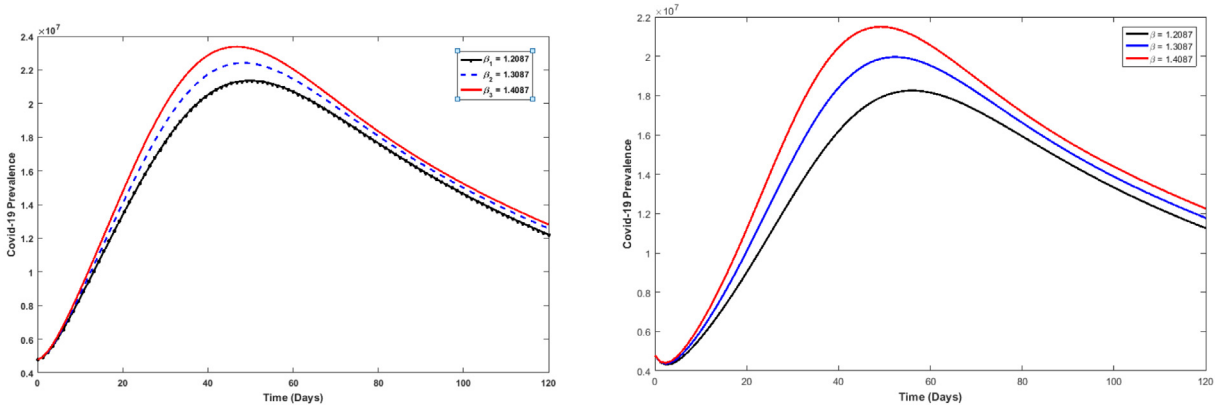


(a) Disease Prevalence when $\mathcal{R}_0 > 1$, when $V = 0$ (b) Disease Prevalence when $\mathcal{R}_0 > 1$, when $V \neq 0$

**Fig. 8.** Covid-19 Disease Prevalence.

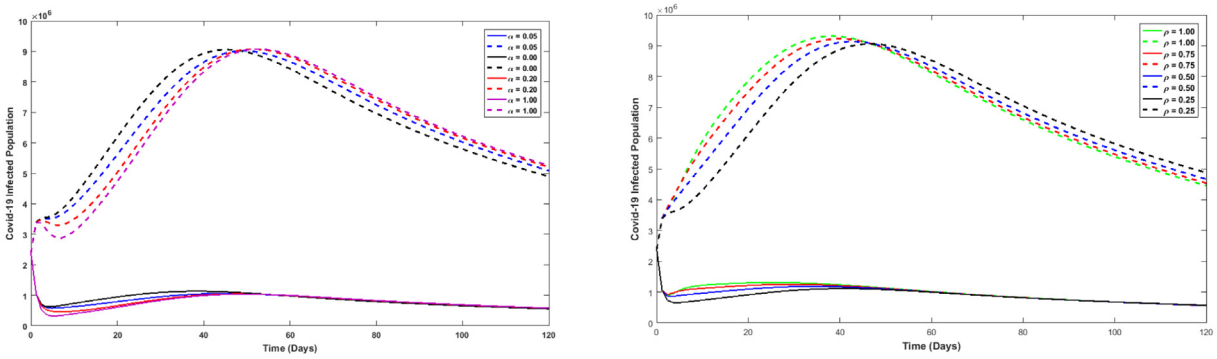


(a) Impact of varying $\alpha$ on infected Compartment (b) Impact of varying $\rho$ on infected Compartment

**Fig. 9.** The Evolutionary Impact of varying $\rho$ and $\alpha$ on the sub-population.

down the progression of pre-symptomatic infected individuals from becoming symptomatic. Similarly, the impact of vaccination was captured in Fig. 9(b) revealing the dynamic behavior of symptomatic and asymptomatic infectious population having varied vaccination rate $\rho$ from 0.25 to 1 which indicates that achieving a vaccination rate of 25% could scale down the growth of both infectious population but have a greater declination with time as the values of $\rho$ increases to 100%.

Aside, other simulations were carried to show the contour plots of the control reproduction number $\mathcal{R}_c$ in terms of some sensitive controllable parameters. So, in Fig. 10 the control $\mathcal{R}_0$ is plotted against some specified model parameters. Hence, Fig. 10(a) reveals the impact of vaccination rate amist immunity loss in the population. Thus, increasing vaccination rate (i.e. Have more people vaccinated) while decreasing the rate at which vaccinated individuals lose their vaccine-derived immunity will result in a decrease in the value of the control reproduction number. This implies that wider vaccination coverage and high vaccine potency are critical factors in eliminating Covid-19 disease in Nigeria. In order to further proffer insight on the impact of vaccination amidst evolution of exposed (Infected) individuals in the population, Fig. 10(b) reveals that nationwide Covid-19 elimination can be achieved (i.e The control reproduction number can be brought below unity) by scaling-up vaccination coverage and enhancing the potency of the vaccines. Also, contact-tracing, regular Covid-19 testing, and early detection of Covid-19 Exposed individuals could help reduce number of individuals in the infectious stage of disease, thus facilitation timely treatment of the patients while equally curtailing the indiscriminate spread of the disease. Similarly, Fig. 10(c) shows a decrease in the value of the reproduction number with increasing vaccination rate and decreasing effective contact rate with infected Covid-19 individuals ($\sigma$), which implies the scaling up vaccination coverage with enforcement of Covid-19 protocols will both work together to drive the epidemic towards extinction. In the same vein, Fig. 10(d) shows that decreasing the effective infection rate with a steady decrease in the vaccine-derived immunity waning rate would result in a remarkable reduction in the control reproduction number below unity and this could eventually lead to the eventual elimination of the disease in the population, particularly in places where adherence to the Covid-19 social protocols is strictly enforced.

## 7. Concluding remarks

An improved deterministic model for the transmission dynamics of novel Coronavirus disease (COVID 19) is developed and rigorously analyzed to proffer insight into the impact of vaccination cum other NPI measures on the spread of dominant alpha strain of the disease in Nigeria. The formulated model incorporates current information on Covid-19 disease such as reinfection after recovery and loss of immunity due to waning. Using the available data from NCDC [11,56,61], the formulated model was fitted to the observed data to estimate best values for some of the unknown parameters. Some of the key results obtained from the model qualitative and quantitative analysis are as follows:

i The proposed model has two equilibria: the Covid-19 disease-extinction equilibrium ($\mathcal{E}_0$)) which is globally-asymptotically stable (GAS) when the basic reproduction number ($\mathcal{R}_o$) is less than unity and the non-extinction equilibrium, ($\mathcal{E}_1$) which is locally asymptotically stable when $\mathcal{R}_{0V} < 1$, which indicates that the proposed model exhibits backward bifurcation due to

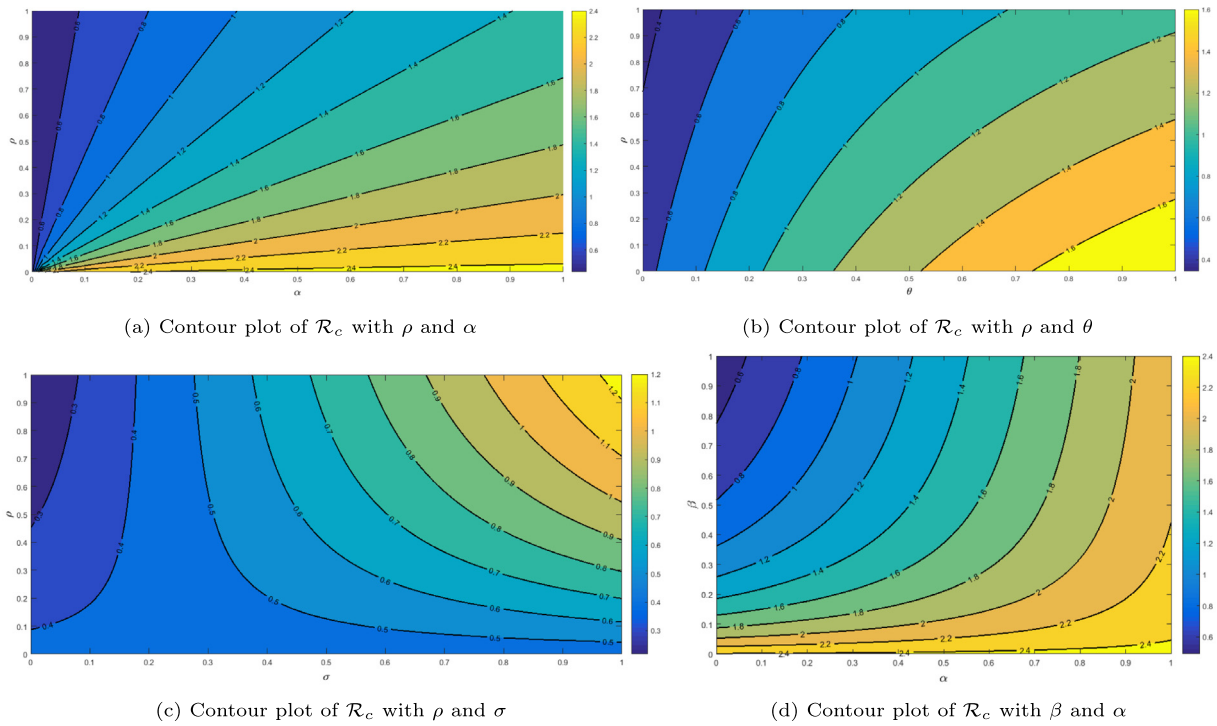

(a) Contour plot of $\mathcal{R}_c$ with $\rho$ and $\alpha$

(b) Contour plot of $\mathcal{R}_c$ with $\rho$ and $\theta$

(c) Contour plot of $\mathcal{R}_c$ with $\rho$ and $\sigma$

(d) Contour plot of $\mathcal{R}_c$ with $\beta$ and $\alpha$

**Fig. 10.** Contour plot of the control reproduction number $\mathcal{R}_c$, as a function of vaccination rate ($\rho$) against fraction of exposed individual ($\theta$), loss of immunity ($\alpha$) and effective contact rate of vaccinated individuals ($\sigma$). The parameter values used to generate the plots are as given in the parameter estimation Table 2.

reinfection of vaccinated individuals who lost their immunity and low vaccination rate.

ii The sensitivity analysis reveals that the effective infection rate of susceptible individuals and progression rate of exposed individuals are most sensitive and positively correlated to the rate of disease transmission, thus making these parameters the targets while adopting measures for the effective control of the spread of the disease.

iii The model simulations show that if the force of infection is reduced significantly amidst vaccination, the reproduction number will be significantly less than unity and this is achievable by adhering strictly to COVID-19 safety measures.

iv The model simulations also reveal that if the effective infection rate can be reduced to at least 40% in the population with about 50% of the populace been vaccinated, then the target of eliminating Corona virus disease is feasible.

## Declaration of competing interest

The authors declare that they have no known competing financial interests or personal relationships that could have appeared to influence the work reported in this paper.

## Data availability

The set of data used and/or analyzed during the current study are available on https://ourworldindata.org/coronavirus/country/Nigeria

## References


[1] D.J. Daley, J. Gani, Epidemic Modelling: An Introduction, Cambridge University Press, Reprinted, 2005.

[2] C.A. Janeway, P. Travers, M. Walport, Immunology: The Immune System in Health and Diseases, fifth ed., Garland Sciences, New York, 2001, Infectious agents and how they cause diseases. https://www.ncbi.nlm.gov/book/NBK27114/.

[3] Nigeria warns of possible new COVID-19 wave, 2020, https://www.voanews.com/africa/nigeria-warns-possible-new-covid-19-wave.

[4] Q. Li, X. Guan, P. Wu, X. Wang, L. Zhou, Y. Tong, et al., Early transmission dynamics in wuhan, China, of novel corona virus infected pneumonia, N. Engl. J. Med. 382 (2020) http://dx.doi.org/10.1056/NEJMoa2001316, 1199e1207.

[5] Statement on the second meeting of the international health regulations, 2005, https://www.who.int/news-room/detail/30-01-2020-statement-on-the-second-meeting-of-the-international-health-regulations-(2005)-emergency-committee-regarding-the-outbreak-of-novel-coronavirus-(2019-ncov).

[6] T.T. Yusuf, I.O. Idisi, Modelling the transmission dynamics of HIV and HBV coepidemics: Analysis and simulation, Math. Theory Model. 10 (2) (2020) 3.

[7] C.N Ngonghala, E. Iboi, S. Eikenberry, M. Scotch, C.R. MacIntyre, M.H. Bonds, A.B. Gumel, Mathematical assessment of the impact of non-pharmaceutical interventions on curtailing the 2019 novel coronavirus, Math. Biosci. (2020) 108364, http://dx.doi.org/10.1016/j.mbs.2020.108364.

[8] H. Harapan, N. Itoh, A. Yufika, W. Winardi, S. Keam, H. Te, D. Megawati, Z. Hayati, A.L. Wagner, M. Mudatsir, Coronavirus disease 2019 (COVID-19): A literature review, J. Infect. Public Health 13 (2020) 667–673, http://dx.doi.org/10.1016/j.jiph.2020.03.019.

[9] WHO coronavirus (COVID-19) dashboard, 2020, Visited 13th November 2020, https://covid19.who.int/.

[10] WHO, Statement on the second meeting of the international health regulations, 2005, https://www.who.int/news-room/detail/30-01-2020.

[11] NCDC Recommendation, Advisory on the use of face masks by members of the public without respiratory symptoms, 2020, Publish May 1 (2020) visited October 2021, https://covid19.ncdc.gov.ng/media/files/UseOfMasks2020_AfMNLz3.pdf.

[12] C. Burrell, C. Howard, F. Murphy, Fenner and White's Medical Virology, fifth ed., Academic Press, United States, 2016, https://scholar.google.com/scholar_lookup?title=Fenner%20and%20White%27s%20medical%20virology&author=C.%20Burrell&publication_year=2016.

[13] J.A. Backer, D. Klinkenberg, J. Wallinga, Incubation period of 2019 novel coronavirus (2019-nCoV) infections among travellers from Wuhan, China, 20–28 January 2020, Eurosurveillence 25 (5) (2020) http://dx.doi.org/10.2807/1560-7917.ES.2020.25.5.2000062, Article pii $\frac{1}{4}$2000062.

[14] B. Tang, X. Wang, Q. Li, N.L. Bragazzi, S. Tang, Y. Xiao, J. Wu, Estimation of the transmission risk of the 2019-nCoV and its implication for public health interventions, J. Clin. Med. 9 (462) (2020) http://dx.doi.org/10.3390/jcm9020462.

[15] Corona-symptoms, 2020, visited June, https://www.who.int/health-topics/coronavirus#tab=tab_3.

[16] A.B. Gumel, E.A. Iboi, C.N. Ngonghala, E.H. Elbasha, A primer on using mathematics to understand COVID-19 dynamics: Modeling, analysis and simulations, Infect. Dis. Model. (2020) http://dx.doi.org/10.1016/j.idm.2020.11.005.

[17] H. Richie, E Ortiz-Ospina, D Beltekian, E Methieu, J. Hasell, B. Macdonald, C. Giattino, C. Appel, L. Rodes-Guirao, M. Roser, 2021, https://ourworldindata.org/covid-vaccinations.

[18] Our World in Data (Visited Dec 2021), https://ourworldindata.org/covid-vaccinations.
[19] Q. Lin, S. Zhao, D. Gao, Y. Lou, S. Yang, S.S. Musa, M.H. Wang, et al., A conceptual model for the outbreak of coronavirus disease 2019 (COVID-19)in Wuhan, China with individual reaction and governmental action, Int. J. Infect. Dis. (93) (2020) http://dx.doi.org/10.1016/j.ijid.2020.02.058.
[20] T.M. Chen, J. Rui, Q.P. Wang, Z.Y. Zhao, J.A. Cui, L. Yin, A mathematical model for simulating the phase-based transmissibility of a novel coronavirus, Infect. Dis. Poverty 9 (1) (2020) http://refhub.elsevier.com/S2468-0427(21)00015-4/sref13.
[21] G. Giordano, F. Blanchini, R. Bruno, P. Colaneri, A. Di Filippo, A. Di Matteo, M. Colaneri, Modelling the COVID-19 epidemic and implementation of population-wide interventions in Italy, Nat. Med. (26) (2020) 855–860, http://dx.doi.org/10.1038/s41591-020-0883-7.
[22] S.E. Eikenberry, M. Mancuso, E. Iboi, T. Phan, K. Eikenberry, Y. Kuang, E. Kostelich, A.B. Gumel, To mask or not to mask: Modeling the potential for face mask use by the general public to curtail the COVID-19 pandemic, Infect. Dis. Model. 5 (2020) http://dx.doi.org/10.1016/j.idm.2020.04.001, 293e308.
[23] M.A. Khan, A. Atangana, Modelling the dynamics of novel coronavirus(2019-ncov) with fractional derivatives, Alexendria Eng. J. (2020) http://dx.doi.org/10.1016/j.aej.2020.02.033.
[24] E.A. Iboi, O.O. Sharomi, C.N. Ngonghala, A.B. Gumel, Mathematical modeling and analysis of COVID-19 pandemic in Nigeria, 2020, http://dx.doi.org/10.1101/2020.05.22.20110387, MedRxiv.
[25] D. Okuonghae, A. Omame, Analysis of a mathematical model for COVID-19 population dynamics in Lagos, Nigeria, Chaos Solitons and Fractals (2020) http://dx.doi.org/10.1016/j.chaos.2020.110032.
[26] Y. Fang, Y. Nie, M. Penny, Transmission dynamics of the COVID-19 outbreak and effectiveness of government interventions: A data-driven analysis, J. Med. Virol. 92 (6) (2020) 645–659.
[27] K. Prem, Y. Liu, T.W. Russell, A.J. Kucharski, R.M. Eggo, N. Davies, S. Flasche, S. Clifford, C.A. Pearson, J.D. Munday, et al., The effect of control strategies to reduce social mixing on outcomes of the COVID-19 epidemic in Wuhan, China: a modelling study, Lancet Publ. Health.
[28] M. Rabiu, S.A. Iyaniwura, Assessing the potential impact of immunity waning on the dynamics of COVID-19 in South Africa: an endemic model of COVID-19, Nonlinear Dynam. 109 (2022) 1.
[29] S.A. Iyaniwura, M. Rabiu, D.K. Jude, A generalized distributed delay model of COVID-19: An endemic model with immunity waning, Math. Biosci. Eng. 20 (3) (2023) 5379–5412.
[30] B. Ivorra, et al., Mathematical modeling of the spread of the coronavirus disease (COVID-19) taking into account the undetected infections. The case of China, Commun. Nonlinear Sci. Numer. Simul. (2019) http://www.doi.org/10.13140/RG.2.2.21543.29604121.
[31] Y. Li, B. Wang, R. Peng, C. Zhou, L. Zhan, Chen, X. Zhuoxun, Jiang, B. Zhao, Mathematical modeling and epidemic prediction of COVID-19 and its significance to epidemic prevention and control measures, Ann. Infect. Dis. Epidemiol. 5 (1) (2020).
[32] Q. Lin, S. Zhao, D. Gao, L. Yinju, Yang Shu, S.S. Musa, H.M. Wang, Y. Cai, W. Wang, L. Yang, Daihai He, A conceptual model for the coronavirus disease 2019 (COVID-19) outbreak in Wuhan, China with individual reaction and governmental action, Int. J. Infect. Dis. (93) (2020) 211–216, http://dx.doi.org/10.1016/j.ijid.2020.02.058.
[33] E.M. Chinwendu, M.A. Nkiru, D. Sambo, The role of mathematical model in curbing COVID-19 in Nigeria, 2020, http://dx.doi.org/10.1101/2020.07.22.20159210, medRxiv preprint.
[34] T.T. Yusuf, A. Abidemi, A.S. Afolabi, E.J. Dansu, Optimal control of the coronavirus pandemic with impacts of implemented control measures, J. Nig. Soc. Phys. Sci. 4 (2022) 88–98, http://dx.doi.org/10.46481/jnsps.2022.414.
[35] I.O. Idisi, Y.T. Oyebo, O.F. Fakoya, V.S. Benson, Y.T. Tunde, A mathematical model for Covid-19 disease transmission dynamics with impact of saturated treatment: modeling, analysis and simulation, Open Access Libr. J. 8 (2021) e7332, http://dx.doi.org/10.4236/oalib.1107332.
[36] E.A. Iboi, C.N. Ngonghala, A.B. Gumel, Will an imperfect vaccine curtail the COVID-19 pandemic in the US? Infect. Dis. Model. (5) (2020) 510e524, http://dx.doi.org/10.1016/j.idm.2020.07.006.
[37] R. Ariana, R. Rachel, E.A. Iboi, Assessment of the COVID-19 vaccine program: impact of the no mask mandate executive order in the state of texas, 2021, http://dx.doi.org/10.1101/2021.04.08.21255156, medRxiv preprint.
[38] A. Boudaoui, Y. El hadj Moussa, Z. Hammouch, S. Ullah, A fractional-order model describing the dynamics of the novel coronavirus (COVID-19) with nonsingular kernel, Chaos Solitons Fractals 146 (2021) (2020) 110859, http://dx.doi.org/10.1016/j.chaos.2021.110859.
[39] Z. Ali, F. Rabiei, M.M. Rashidi, T. Khodadadi, A fractional-order mathematical model for COVID-19 outbreak with the effect of symptomatic and asymptomatic transmissions, The Eur. Phys. J. Plus 137 (3) (2022) 1–20.
[40] A. Alam Khan, A. Rohul, U. Saif, S. Wojciech, A. Mohamed, Numerical simulation of a Caputo fractional epidemic model for the novel coronavirus with the impact of environmental transmission, Alexandria Eng. J. (61) (2022) 5083–5095, http://dx.doi.org/10.1016/j.aej.2021.10.008.
[41] Ndolane Sene, Fractional SIRI model with delay in context of the generalized Liouville-Caputo fractional derivative, Math. Model. Soft Comput. Epidemiol. (2020) 107–125.
[42] Ndolane Sene, SIR epidemic model with Mittag-Leffler fractional derivative, Chaos Solitons Fractals 37 (2020) 09833, http://dx.doi.org/10.1016/j.chaos.2020.109833.
[43] M. Weiyuan, Z. Yanting, G. Lihong, C. YangQuan, Qualitative and quantitative analysis of the COVID-19 pandemic by a two-side fractional-order compartmental model, ISA Trans. 124 (2022) 144–156, http://dx.doi.org/10.1016/j.isatra.2022.01.008.
[44] A. Sadia, K. Sadia, J. Sana, A. Naima, N. Fariha, Modeling the impact of the vaccine on the COVID-19 epidemic transmission via fractional derivative, Eur. Phys. J. Plus 137 (2022) 802, http://dx.doi.org/10.1140/epjp/s13360-022-02988-x.
[45] S. Murugesan, S. Sriramulu, G. Vediyappan, U. Fernandez-Gamiz, N. Samad, Stability analysis of COVID-19 outbreak using Caputo–Fabrizio fractional differential equation, AIMS Math. 8 (2) (2022) 2720–2735, http://dx.doi.org/10.3934/math.2023143.
[46] O.O. Okundalaye, W.A.M. Othman, A.S. Oke, Toward an efficient approximate analytical solution for 4-compartment COVID-19 fractional mathematical model, J. Comput. Appl. Math. 416 (2022) (2022) 114506, http://dx.doi.org/10.1016/j.cam.2022.114506.
[47] S.S Amjad, N.S. Iqbal, S.N. Kottakkaran, A mathematical model of COVID-19 using fractional derivative: outbreak in India with dynamics of transmission and control, Adv. Difference Equ. (2020) 373, http://dx.doi.org/10.1186/s13662-020-02834-3.
[48] P. Kumar, S.E. Vedat, m. Murillo-Arcila, A new fractional mathematical modelling of COVID-19 with the availability of vaccine, Results Phys. 24 (2020) (2021) 104213, http://dx.doi.org/10.1016/j.rinp.2021.104213, 373.
[49] Z. Zizhen, A novel covid-19 mathematical model with fractional derivatives: Singular and nonsingular kernels, Chaos Solitons Fractals 139 (2020) 110060, http://dx.doi.org/10.1016/j.chaos.2020.110060.
[50] H. Khan, F. Ahmad, O. Tunc, M. Idrees, On fractal-fractional Covid-19 mathematical model, Chaos Solitons Fractals 157 (2022) 111937.
[51] P. Lynne, Covid reinfections likely within one or two years, model purpose, Nat. Med. (2021) http://dx.doi.org/10.1038/d41586-021-02825-8.
[52] S. Lakshmikantham, S. Leela, A.A. Martynyuk, Stability Analysis of Nonlinear Systems, Marcel Dekker, Inc., New York, 1989.
[53] I.O. Idisi, T.T. Yusuf, A mathematical model for lassa fever transmission dynamics with impacts of control measures: analysis and simulation, EJ-Math. 2 (2) (2021) http://dx.doi.org/10.24018/ejmath.2021.2.2.17.
[54] J. Lassale, S. Lefschetz, The Stability of Dynamical System, SIAM Philadelphia, 2010.
[55] P. Van Den Driessche, J. Watmough, Reproduction numbers and sub-threshold endemic equilibria for compartmental models of disease transmission, Math. Biosci. (180) (2002) 29–48.
[56] U. Danbaba, S. Garba, Stability analysis and optimal control for yellow fever model with vertical transmission, Int. J. Appl. Comput. Math. 6 (2020) 105, http://dx.doi.org/10.1007/s40819-020-00860-z.
[57] C. Castillo-Chavez, B. Song, Dynamical models of tuberculosis and their applications, Math. Biosci. Eng. 2 (2004) 361–404.
[58] Worldometer, Covid-19 corona virus pandemic, 2021, https://github.com/owid/covid-19data/tree/master/public/data, Visited: March 17, 2022.
[59] WHO, Latest WHO disease outbreak news (DONs), 2021, https://www.who.int/emergencies/disease-outbreak-news/1.
[60] S. Marino, I.B. Hogue, C.J. Ray, D.E. Kirschner, A methodology for performing global uncertainty and sensitivity analysis in systems biology, J. Theoret. Biol. 254 (1) (2008) 178–197.
[61] Novel Coronavirus (COVID-19), Situation Dashboard, Center for Disease Control and Prevention https://experience.arcgis.com/experirnce/685d0ace521648f8a5beeeee1b9125cd.